OPEN ACCESS Freely available online

Immunotherapy: Open Access

Research Article

A Comprehensive Pan-Cancer Analysis of Obg-like ATPase 1 (*OLA1*): A Prognostic and Immunological Biomarker

Jian-Kun Zhang[1,3,4], Lu-Yang Zou[2,3,4], Yi-Yi Cai[3,4], Yue Liu[3,4], Xin-Yu Chen[5], Yi-Wen Wu[6], Dong Xu[3,4*]

[1]Department of Gastroenterology Surgery, Shaoxing University, Shaoxing, Zhejiang, China; [2]Department of Gastroenterology Surgery and Oncology, Sichuan University, Yibin, Sichuan, China; [3]Department of Colorectal Surgery and Oncology, Zhejiang University School of Medicine, Hangzhou, Zhejiang, China; [4]Department of Oncology, Zhejiang University, Hangzhou, Zhejiang, China; [5]Department of Urology, School of Medicine, Shanghai Jiao Tong University, Shanghai, China; [6]Department of Neurosurgery, Zhejiang University School of Medicine, Hangzhou, Zhejiang, China

ABSTRACT

Objective: Obg-like ATPase 1 (*OLA1*) is reported to influence tumorigenesis and development in a few particular cancer types, while there has not been an integrated analysis of *OLA1* in pan-cancer.

Methods: *OLA1* expression differences between tumor and normal tissues were explored based on The Cancer Genome Atlas Program (TCGA) and Genotype-Tissue Expression (GTEx) databases. Next, Cox regression and Kaplan-Meier analyses were used to assess the relationship between *OLA1* expression and prognosis. Further, the correlation between *OLA1* expressions with Tumor Mutational Burden (TMB), Microsatellite Instability (MSI), Copy Number Variation (CNVs) and Deoxyribonucleic acid (DNA) methylations were also investigated respectively. In addition, Tumor IMmune Estimation Resource (TIMER2.0), Gene Set Cancer Analysis (GSCA), Tumor Immune System Interactions Database (TISIDB) and Tumor Immune Syngeneic Mouse (TISMO) were applied for detecting the immune and drug aspects of *OLA1*. Moreover, Gene Ontology (GO) and Kyoto Encyclopedia of Genes and Genomes (KEGG) enrichment analyses were utilized to predict signaling pathways and the Protein-Protein Interaction (PPI) networks were established by GeneMultiple Association Network Integration Algorithm (GeneMANIA) and Search Tool for the Retrieval of Interacting Genes/Proteins (STRING).

Results: *OLA1* had abnormal expressions in 28 of 33 TCGA tumors. Increased or decreased *OLA1* expression levels were connected with Overall Survival (OS), Disease-Specific Survival (DSS), Progression-Free Survival (PFS) and Disease Free Interval (DFI) in different malignancies. *OLA1* expressions had positive correlations with 12 tumors of TMB and 22 of CNV. Conversely, the negative relationships were found in 7 cancer types of MSI and 8 of methylation. Moreover, we demonstrated that *OLA1* expressions were negatively associated with Cancer-Associated Fibroblasts (CAF), macrophage and endothelial cells in Colon Adenocarcinoma (COAD) and Lung Squamous Cell Carcinoma (LUSC) by multiple algorithms. Meanwhile, *OLA1* had negative correlations with immune, stromal and estimate scores in most cancers, such as LUSC, Lower Grade Glioma (LGG) and Tetrahydrocannabinolic Acid (THCA). Additionally, *OLA1* was shown significantly connections with a variety of immunoregulation-related genes and immune checkpoints. *OLA1* could also predict immunotherapy response in 5 murine immunotherapy cohorts. Further, enrichment analyses showed that *OLA1* was involved in cell cycle, DNA replication origin binding, DNA combination and others, which affected tumorigenesis.

Conclusion: *OLA1* was aberrantly expressed in multiple cancer types and related to patient outcomes, immune infiltration and genetic alteration aspects. Hence, *OLA1* may be a potential immunological and prognostic biomarker in pan-cancer.

Keywords: *OLA1*; Pan-cancer, Tumor microenvironment; Immunotherapy; Prognosis; Biomarker

Correspondence to: Dong Xu, Department of Colorectal Surgery and Oncology, Zhejiang University School of Medicine, Hangzhou, Zhejiang, China, E-mail: xudongzju@gmail.com

Received: 21-Nov-2024, Manuscript No. IMT-24-35295; **Editor assigned:** 25-Nov-2024, PreQC No. IMT-24-35295 (PQ); **Reviewed:** 10-Dec-2024, QC No. IMT-24-35295; **Revised:** 17-Dec-2024, Manuscript No. IMT-24-35295 (R); **Published:** 24-Dec-2024, DOI: 10.35248/2471-9552.24.10.265

Citation: Zhang JK, Zou LY, Cai YY, Liu Y, Chen XY, Wu YW, et al (2024). A Comprehensive Pan-Cancer Analysis of Obg-like ATPase 1 (*OLA1*): A Prognostic and Immunological Biomarker. Immunotherapy (Los Angel). 10:265.

Abbreviations: CTRP: Genomics of Therapeutics Response Portal; EMT: Epithelial-Mesenchymal Transition; ESCA: Esophageal Cancer; ESTIMATE: Estimation of STromal and Immune cells in MAlignant Tumors using Expression data; GEPIA2: Gene Expression Profiling Interactive Analysis; HNSC: Head and Neck Squamous Cell Carcinoma; HPA: The Human Protein Atlas; HR: Hazard Ratio; IC_{50}: Drug half maximal inhibitory concentration; RASMAPK: RAS-Mitogen-Activated Protein Kinase

INTRODUCTION

Cancer is a leading cause of death and an essential obstacle to increase the quality of life all over the world, regardless of the level of human development. Despite the fact that there are plenty of methods for controlling the circumstances, the outcomes fall short of expectations. Immunotherapy, specifically immune checkpoint blocking therapy, has recently become a hot spot in tumor treatment. Benefiting from the ongoing development of these open-access databases, such as TCGA and Human Protein Atlas (HPA), it is now possible to identify some new immunotherapy targets by performing pan-cancer gene expression analysis, evaluating their correlations with clinical prognosis and potential related signaling pathways [1,2].

OLA1 is an unconventional member that can hydrolyze Adenosine Triphosphate (ATP) more efficiently than Guanine TriPhosphate (GTP), which belongs to the Obg-like family and YchF subfamily of P-loop GTPases. *OLA1* is universally conserved from prokaryotes to eukaryotes, which performs numerous kinds of essential functions in many cellular processes, specifically in cell division. As previous researches reported, *OLA1* engaged in the regulation of cellular proliferation during the cell cycle. Moreover, *OLA1* has been reported being overexpressed in several human malignancies, which has influences on Epithelial-Mesenchymal Transition (EMT) *via* different mechanisms. Recently, *OLA1* has been identified as a molecular biomarker with prognostic and therapeutic potential for Uterine Corpus Endometrial Carcinoma (UCEC). According to the findings above, *OLA1* is an influential gene in a variety of human malignancies. However, most researches on the functions of *OLA1* in tumorigenesis and developments have been limited to a few particular cancer types. There has not been a pan-cancer analysis of *OLA1* in various malignancies [3-13].

In our study, multiple databases were used to explore the expression and prognosis differences of *OLA1* in normal and tumor tissues, such as TCGA, HPA, the GTEx dataset and others. We also evaluated the latent associations between *OLA1* and immune infiltration and genetic alteration aspects. Further, we used the TISMO to explore *OLA1* expression and the Immune Checkpoint Blockade (ICB) treatment effects in mice. Moreover, the GSCA platform was applied for investigating the drug sensitivity. Our results demonstrated that *OLA1* could be considered as a prognostic factor for a range of cancers and that *OLA1* contributed to tumor immunity by affecting tumor infiltrating immune cells. Our study first performed an integrated analysis of *OLA1* in pan-cancer, which uncovered an insightful role of *OLA1* in Tumor Microenvironment (TME) and immunotherapy.

MATERIALS AND METHODS

OLA1 gene expression analyses based on multiple databases

The *OLA1* gene Ribonucleic Acid (RNA)-seq data of pan-cancer samples were obtained from TCGA database on Genomic Data Commons (GDC), which including Adrenocortical Carcinoma (ACC), Bladder Cancer (BLCA), Breast Carcinoma (*BRCA*), Cervical Squamous Cell Carcinoma and Endocervical Adenocarcinoma (CESC), Cholangiocarcinoma (CHOL), COAD, Diffuse Large B-Cell lymphoma (DLBC), Esophageal Cancer (ESCA), Glioblastoma (GBM), Head and Neck Squamous Cell Carcinoma (HNSC), Kidney Chromophobe (KICH), Kidney Renal Clear Cell carcinoma (KIRC), Kidney Renal Papillary cell carcinoma (KIRP), Acute Myeloid Leukemia (LAML), LGG, Liver Hepatocellular Carcinoma (LIHC), Lung Adenocarcinoma (LUAD), LUSC, Mesothelioma (MESO), Ovarian serous cystadenocarcinoma (OV), Pancreatic Adenocarcinoma (PAAD), Pheochromocytoma and Paraganglioma (PCPG), Prostate Cancer (PRAD), Rectal Cancer (READ), Sarcoma (SARC), Skin Cutaneous Melanoma (SKCM), Stomach Adenocarcinoma (STAD), Testicular Germ Cell Tumor (TGCT), Thyroid Carcinoma (THCA), Thymoma (THYM), UCEC, University of California Santa Cruz (UCSC) and Uveal Melanoma (UVM). The Gene Expression Profiling Interactive Analysis (GEPIA2) module was used to analyze the relationship between *OLA1* expression and pathological stages in different tumors. The normal tissue samples data about RNA and protein levels came from the GTEx dataset and HPA dataset respectively. Immunohistochemistry (IHC) images of *OLA1* protein expression in 4 normal tissues and matched tumor tissues, including LUSC, LUAD, Colorectal Cancer (COADREAD) and LGG and Glioblastoma and Lower Grade Glioma (GBMLGG), were downloaded from the HPA and analyzed. The cell lines data of *OLA1* expression were also from the HPA dataset. Using information from the TISIDB website we gathered *OLA1* expression data for various molecular subtypes of tumors and those with notable expression differences were displayed [14-18].

Correlation of *OLA1* expression with prognosis

Survival data of pan-cancer were downloaded from UCSC, TCGA datasets and a standardized dataset named TCGA pan-cancer Clinical Data Resource (TCGA-CDR). We chose OS, Disease-Specific Survival (DSS), Progression Free Survival (PFS) and Disease-Free Interval (DFI) to explore the relationship between *OLA1* expression and patient prognosis. Cox regression analyses were used to assess the relationship between *OLA1* expression and OS, DSS, PFS and DFI of patients. We used the Kaplan-Meier (KM) curves to demonstrate the difference between "high" and "low" risk groups based on the best separation of *OLA1* expression. Moreover, we investigated the association between *OLA1* Gene Set Variation Analysis (GSVA) score with patient survival on GSCA website. *OLA1* GSVA score represents the integrated level of the expression of *OLA1* gene set, which positively correlated with *OLA1* expression and calculated by R package GSVA [19-21].

OLA1-associated genetic alteration analyses and prognosis

The mutation status of *OLA1* in all TCGA tumors was examined using the cBio Cancer Genomics Portal (cBioPortal), with an emphasis on the frequency, alteration type and mutation site.

To evaluate the *OLA1*-associated genetic alteration with patient prognosis in pan-cancer, we simultaneously gathered the survival data, OS, DFI, DSS and PFS. To investigate the *OLA1* expression correlated with Tumor Mutational Burden (TMB) and MSI in pan-cancer, we calculated the TMB and MSI scores based on the data from UCSC, GDC and a previous study. The correlation between *OLA1* expression and MSI and TMB was examined, which results were shown in the lollipop charts. Moreover, GSCA website was used to study the *OLA1* expression associated with CNV and DNA methylation across all TCGA tumors, the corresponding prognosis with *OLA1* CNV/gene set CNV and methylation levels were also explored. All of the results were performed in the bubble plots [22-24].

Immune aspects of *OLA1* in the tumor microenvironment

TIMER2.0 tool was used to analyze the relationship between *OLA1* expression and immune cell infiltration in pan-cancer. Tumor Immune Estimation Resource (TIMER), Estimation of the Proportions of Immune and Cancer cells (EPIC), Tumor Immune Dysfunction and Exclusion. (TIDE), Cross-platform Cell-type Enrichment Analysis (XCELL) and Microenvironment Cell Populations-counter (MCP-counter) algorithms were applied for the correlation analyses of the levels of CAF, Macrophages (Mφ) and Endothelial Cells (EC) and the expression levels of *OLA1*. We also detected the correlations between *OLA1* GSVA scores and 24 immune cell infiltrations from Immune Cell Abundance Identifier (ImmuCellAI) based on GSCA [20]. Moreover, the Estimation of STromal and Immune cells in MAlignant Tumors using Expression data (ESTIMATE) method was utilized to calculate immune, stromal and estimate scores for each tumor sample based on TCGA and GTEx databases. Following that, we evaluated the associations between *OLA1* expressions and three scores above by Spearman correlation analyses. In addition, we used TISIDB website to explore the associations between *OLA1* expressions and different tumor immune subtypes [18]. Further, we performed co-expression spearman analyses on *OLA1* and immunoregulation genes and immunological checkpoints in pan-cancer [25-30].

Immunotherapy and drug response analysis of *OLA1*

TISMO and GSCA websites were used to forecast the immunotherapy and drug responses of *OLA1* [20,31]. We collected the drug half maximal Inhibitory Concentration (IC_{50}) and their corresponding *OLA1* mRNA expression data from Genomics of Drug Sensitivity in Cancer (GDSC) and Genomics of Therapeutics Response Portal (CTRP). The top 30 medications in terms of ranking were displayed in bubble plots as we investigated the relationship between *OLA1* expression and drug IC_{50}.

OLA1-related enrichment analyses and PPI networks

To probe *OLA1*-related genes, we performed the pearson correlation analysis based on all TCGA tumor and normal tissues datasets through GEPIA2 "similar" module [15]. The top 100 genes positively associated with *OLA1* were selected to perform the GO analysis and KEGG pathway enrichment analysis. Further, Search Tool for the Retrieval of Interacting Genes/Proteins (STRING) was used to explore *OLA1*-binding experimentally PPI network. We set the main parameters as follows: Network type (full STRING network), minimum required interaction score (medium confidence (0.400)) active interaction sources (experiments) and max number of interactions to show (no more than 10 interactions). We also investigated the PPI of *OLA1* by Gene Multiple Association Network Integration Algorithm (GeneMANIA) platform. In addition, we explored the relationship between *OLA1* protein levels and pathway activities by GSCA platform [32-35].

Statistical analysis

The connection between *OLA1* expression or *OLA1* GSVA score and each target of interest, including *OLA1* similar genes, immune cell infiltration (calculated by multiple algorithms), immune score, stromal score, estimate score, immunoregulation-related genes, immune checkpoints, TMB, MSI, CNV, DNA methylation and drug IC_{50}, was evaluated by Spearman or Pearson correlation analysis. Student t test was used to detect the correlation between *OLA1* expression or *OLA1* GSVA score and pathway activity. Wilcoxon rank sum test or Wilcoxon signed rank test were used to compare *OLA1* expression across groups or between tumor and normal tissues, according to the samples whether pair or not. Based on different statistical methods, p value or False Discovery Rate (FDR) ≤ 0.05 was considered as statistically significant. Cox regression and Kaplan-Meier analysis were used to study the relationship between expression level, GSVA score, CNV, gene set CNV, methylation of *OLA1* and patient prognosis, such as OS, DSS, DFI and PFS. Cox p-value, log-rank p-value, Hazard Ratio (HR) and 95% Confidence Intervals (CI) were examined and the p-value<0.05 was significant. The R software (3.6.3 version) and several online tools (HPA, GEPIA2, TISIDB, GSCA, GeneMANIA, STRING, TIMER2.0, cBioPortal, TISMO, GTEx) were used in our study.

RESULTS

Expression profile of *OLA1* in pan-cancer

To explore the mRNA expression level of *OLA1* in normal tissues, we used the HPA and GTEx datasets. In 51 normal tissues from HPA dataset, the results showed that *OLA1* expressions were the highest in skeletal muscle and tongue tissues compared to other tissues, while the lowest expressions of *OLA1* were found in lung and spleen tissues compared with others. In 54 normal tissues from GTEx dataset, we found that the highest *OLA1* mRNA expression tissue is "EBV-transformed lymphocytes", while the lowest one is "whole blood". Meanwhile, we also probed the *OLA1* protein expression level in normal tissues using HPA. HPA provided the overview of *OLA1* protein expressions in 44 normal tissues and the expression scores were classified three grades, low, medium and high. The results demonstrated that the lowest *OLA1* protein expressions were found in heart muscle, soft tissues and adipose tissues compared to other normal tissues. After that, we used the HPA RNA-seq dataset to evaluate the *OLA1* mRNA expression in 69 tissue culture cell lines. Data from HPA revealed that the top five *OLA1* mRNA enriched cell lines were Prostate Cancer-3 (PC-3), Non-Transformer Bone Marrow 4 (NB-4), Human Leukemia 60 (HL-60), Karyotype 562 (K-562) and Daudi.

Next, TCGA cohorts and GTEx datasets were used to analyze the mRNA expression of *OLA1* in pan-cancer. The results indicated that *OLA1* significantly increased in BLCA, *BRCA*, CESC, CHOL, COAD, DLBC, ESCA, GBM, HNSC, KIRC, KIRP, LGG, LIHC, LUAD, LUSC, OV, PAAD, PRAD, READ, SKCM, STAD, TGCT, THCA, THYM, UCEC and UCS tissues than normal control tissues (Figure 1A, p<0.001). However, there was no significance

in ACC and PCPG (Figure 1A, p>0.05). In particular, *OLA1* upgraded in BLCA, *BRCA*, CHOL, COAD, ESCA, HNSC, KIRC, LIHC, LUAD, LUSC, PRAD, READ, STAD, UCEC tumor samples than paired normal controls, but downgraded in KICH (Figure 1B, p<0.05) (Figures 1A-1H).

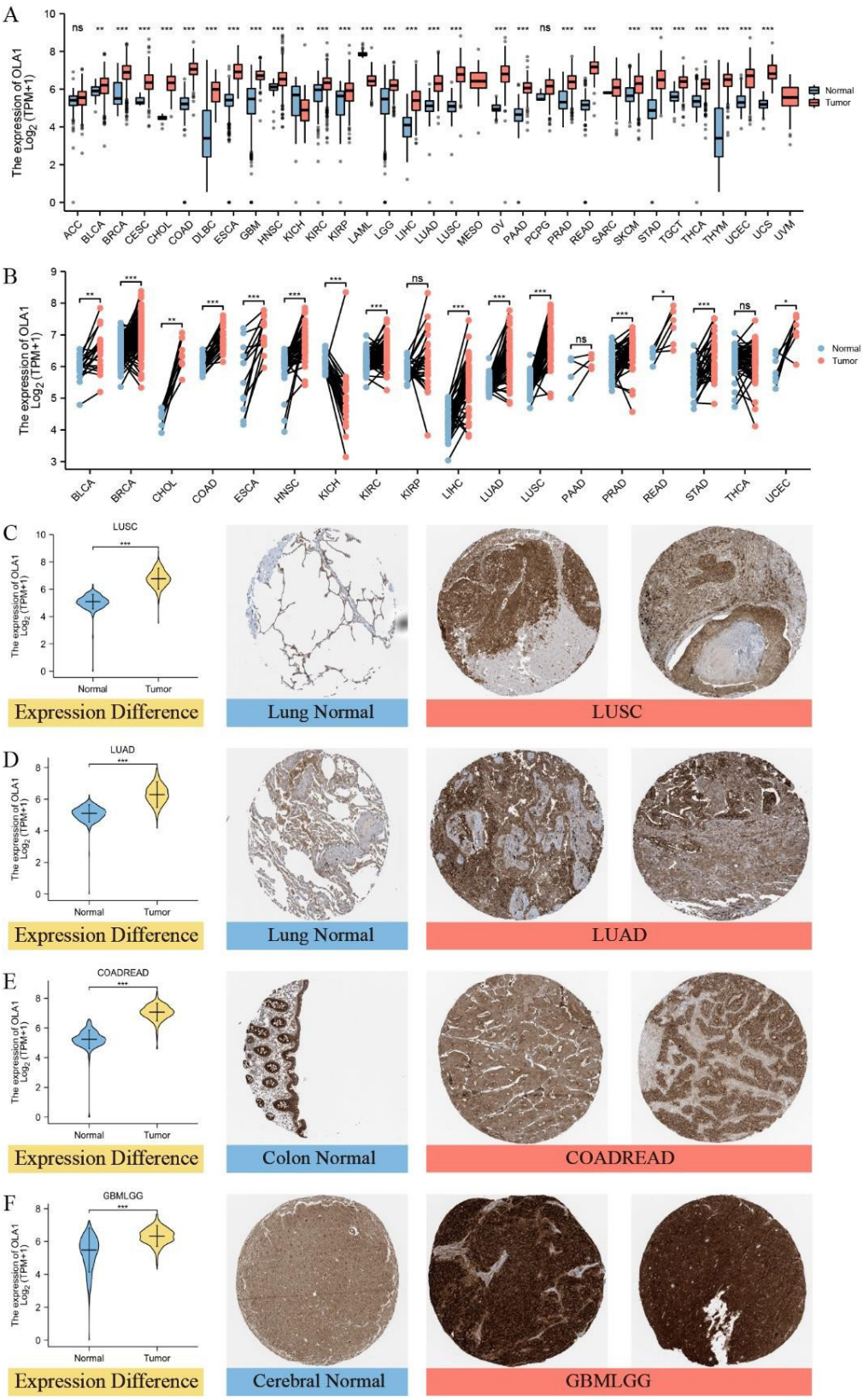

Figure 1: Aberrant expression of Obg-like ATPase 1 (*OLA1*) gene in pan-cancer. **Note:** A) Expression landscape of Obg-like ATPase 1 (*OLA1*) between tumor tissues from The Cancer Genome Atlas (TCGA) database and normal tissues from TCGA and Genotype-Tissue Expression (GTEx) database; B) *OLA1* expression in different tumor and paired normal tissues based on TCGA cohort; C) Lung Squamous Cell Carcinoma (LUSC); D) Lung Adenocarcinoma (LUAD); E) Colorectal Cancer (COADREAD); C-F) Comparison of *OLA1* expression between normal and tumor tissues (left) and immunohistochemistry in normal (middle) and tumor (right) tissues. The top four tumors with the most notable expression differences.

We also explored the relationship between *OLA1* mRNA expression and pathological stages in TCGA tumors by using the GEPIA2 tool, which indicated stage-specific expressional variations in *OLA1* expression in case of a few cancer types, such as KICH, KIRP, LIHC and LUAD (Figures 2A-2D, p<0.05). In other cancer types, there was no significantly correlation between *OLA1* and pathological stages. In addition, we used TISIDB to perform another analysis to investigate the association between *OLA1* expression with cancer molecular type, which results showed that *OLA1* expression was significantly correlation with LGG, OV, HNSC, STAD, KIRP, LUSC and UCEC (Figures 2E-2H, p<0.05), other cancers were shown.

To assess the *OLA1* expression at protein level, we analyzed IHC images from HPA and compared the results with *OLA1* mRNA expression data from TCGA. We found that the results from two databases were unanimous. LUSC, LUAD, COADREAD and GBMLGG were top four tumors with the most notable mRNA expression differences and these four tumors also had stronger IHC staining than corresponding normal tissues. To sum up, *OLA1* expression was elevated in lots of cancer types compared with corresponding normal tissues and *OLA1* might be an oncogene in cancers above.

OLA1 expression levels are associated with patient prognosis across cancers

To explore the relationship between *OLA1* expression level and patient prognosis, we performed a survival analysis across all TCGA tumors, OS, DSS, PFS, DFI were chosen as the indicators for use. Cox proportional-hazard model analysis showed that *OLA1* expression levels were correlated with OS in LIHC (p<0.001), LUAD (p<0.001), KIRP (p<0.01), HNSC (p<0.01), ACC (p<0.01), MESO (p<0.01), PAAD (p<0.05), LGG p<0.05), CESC (p<0.05) and KIRC (p<0.05) (Figure 2A).

Interestingly, high *OLA1* expression was associated with a poor prognosis in LIHC (HR=1.89), LUAD (HR=1.52), KIRP (HR=1.91), HNSC (HR=1.37), ACC (HR=2.29), MESO (HR=1.75), PAAD (HR=1.82), LGG (HR=1.70) and CESC (HR=1.66), but linked with a well prognosis in KIRC (HR=0.71). Kaplan-Meier analysis also suggested that among the patients who with ACC, HNSC, LIHC, LUAD and MESO, those with high *OLA1* expression levels were associated with poor OS, while in patients with KIRC, high *OLA1* expression had a longer survival time (Figures 2C-H, p<0.01). Kaplan-Meier curves of OS in other malignancies were demonstrated (Figures 2A-2H).

In addition, Cox regression analysis of DSS showed that high *OLA1* expression levels were significantly associated with poor prognosis in LIHC (p<0.001, HR=2.00), KIRP (p<0.001, HR=2.59), LUAD (p<0.01, HR=1.60), HNSC (p<0.01, HR=1.49), ACC (p<0.01, HR=2.16), PAAD (p<0.05, HR=1.85), CESC (p<0.05, HR=1.80), LGG (p<0.05, HR=1.66), MESO (p<0.05, HR=1.67). On the contrary, in KIRC (p<0.001, HR=0.61), low expression of *OLA1* was associated with poor DSS (Figure 3A). Kaplan-Meier analysis exhibited a correlation between low *OLA1* expressions and longer DSS among the patients with MESO, HNSC, LIHC, LUAD and KIRP, however, high *OLA1* expression indicated the KIRC patients might have a better prognosis (p<0.001). KM curves of DSS in other cancers were performed (Figures 3A-3H).

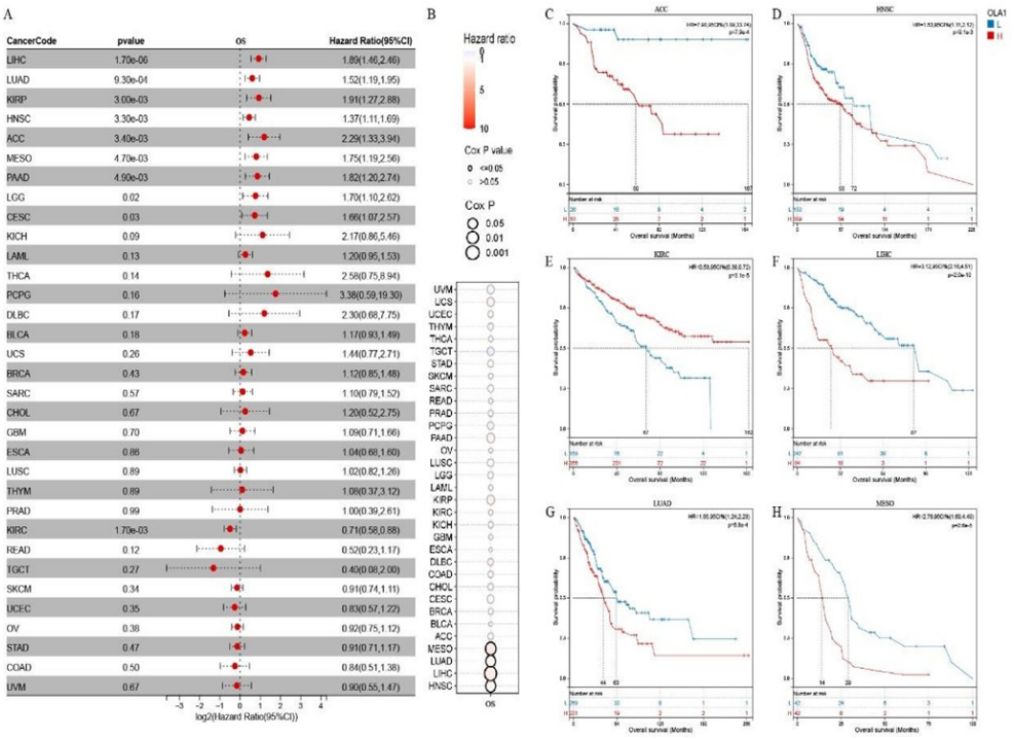

Figure 2: Correlation between *OLA1* expression level and Overall Survival (OS) in The Cancer Genome Atlas (TCGA) tumors. **Note:** A) Forest map shows the univariate Cox regression results of Obg-like ATPase 1 (*OLA1*) for OS in tumors from TCGA database; B) Bubble plot shows the relationship between *OLA1* Gene Set Variation Analysis (GSVA) score and OS by performing the Cox Proportional-Hazard model; C-H) Kaplan-Meier curves shows the expression of *OLA1* in 6 TCGA tumors most significantly associated with OS (p<0.01).

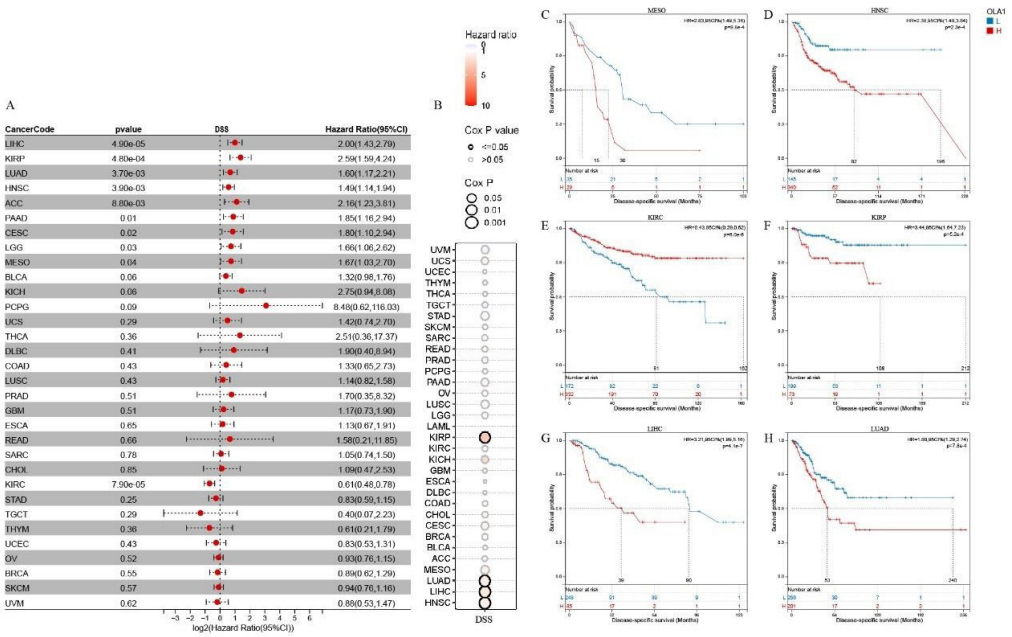

Figure 3: Correlation between Obg-like ATPase 1 (*OLA1*) expression level and Disease-Specific Survival (DSS) in The Cancer Genome Atlas (TCGA) tumors. **Note:** A) Forest map shows the univariate Cox regression results of *OLA1* for DSS in tumors from TCGA database; B) Bubble plot shows the relationship between *OLA1* Gene Set Variation Analysis (GSVA) score and DSS by performing the Cox Proportional-Hazard model; C-H) Kaplan-Meier curves shows the expression of *OLA1* in 6 TCGA tumors most significantly associated with DSS (p<0.001).

Moreover, regarding connection between *OLA1* expression and PFS, a forest plot revealed associations between high expression and poor PFS in ACC (p<0.001, HR=2.66), LIHC (p<0.001, HR=1.50), KIRP (p<0.01, HR=1.93), HNSC (p<0.01, HR=1.36), PAAD (p<0.05, HR=1.68), LUAD (p<0.05, HR=1.30) and CESC (p<0.05, HR=1.56), while low *OLA1* expression was associated with poor PFS in KIRC (p<0.05, HR=0.76) and STAD (p<0.05, HR=0.75) (Figure 4A). KM analysis indicated a correlation between high expression of *OLA1* and poor PFS in patients with ACC, LUAD, HNSC, KIRP and LIHC, but it associated with a longer PFS in KIRC individuals (Figures 4C-4H, p<0.01). KM curves of PFS in other tumors were shown (Figures 4A-4H).

Furthermore, the relationship between *OLA1* expression and DFI was also analyzed by Cox analysis. The results demonstrated that upgraded *OLA1* expressions were connected with shorter DFI among the patients with PAAD (p<0.01, HR=3.50), LIHC (p<0.01, HR=1.39), CESC (p<0.01, HR=2.61), ACC (p<0.05, HR=3.16), however, it associated with a longer DFI in STAD (p<0.05, HR=0.56) (Figure 5A). By Kaplan-Meier analysis, we found that high *OLA1* expression levels were correlated with poor DFI in ACC, PAAD, LIHC, PCPG and CESC, but in STAD, *OLA1* expression showed an opposite effect on prognosis (Figures 5C-5H, p<0.05). KM curves of DFI in other cancers were displayed. (Figures 5A-5H).

Finally, we investigated the association between *OLA1* GSVA score and patient survival based on GSCA website. GSVA score represents the variation of gene set activity over a specific cancer's sample population in an unsupervised manner. In other words, *OLA1* GSVA score represents the integrated level of the expression of gene set, which is positively correlate with *OLA1* gene expression. Cox proportional-hazard model analysis indicated that higher *OLA1* GSVA score was associated with poor OS in MESO, LUAD, LIHC and HNSC (Figure 2B, p<0.05). For DSS data, among patients with KIRP, LUAD, LIHC and HNSC, higher *OLA1* GSVA score had significantly correlation with shorter DSS (Figure 3B, p<0.05). Data from PFS indicated that higher *OLA1* GSVA score was associated with poor PFS in KIRP, MESO, LIHC and HNSC patients (Figure 4B, p<0.05). No correlation was detected between *OLA1* GSVA score and DFI in any cancer types (Figure 5B, all p>0.05).

OLA1 genetic alteration analyses in pan-cancer

The accumulating number of genetic alterations is intimately associated with tumor development. Therefore, we explored the *OLA1* genetic alterations status across TCGA cancers by cBioPortal website. Based on our results, the frequency of *OLA1* alteration (~3%) is the highest in head and neck cancer with "amplification" as the primary type. CHOL had the highest incidence (2~3%) of "structural variant" type and endometrial cancer had the highest alteration frequency (2~3%) of "mutation" type respectively (Figure 6A). Further, we displayed additional mutations with their sites of *OLA1* in Figure 6B. 69 mutations were detected from TCGA database, which including 55 missense, 8 truncating, 1 inframe, 1 splice and 4 fusion. According to our results, we found that R137C was the most frequent mutation site in TCGA cancers (3/69), which altered in three cancer types, *BRCA*, LUSC and UCEC. In addition, COADREAD was the cancer which had the largest number of *OLA1* mutations (9/69). In order to explore whether there was a connection between *OLA1* alterations and patient prognosis, we developed and correlated these across TCGA tumors. In LIHC, patients with *OLA1* alterations indicated a poor prognosis, including OS (p<0.05), DSS (p<0.001), DFI (p<0.01), PFS (p<0.001), compared with patients without alterations of *OLA1* (Figures 6A-6F).

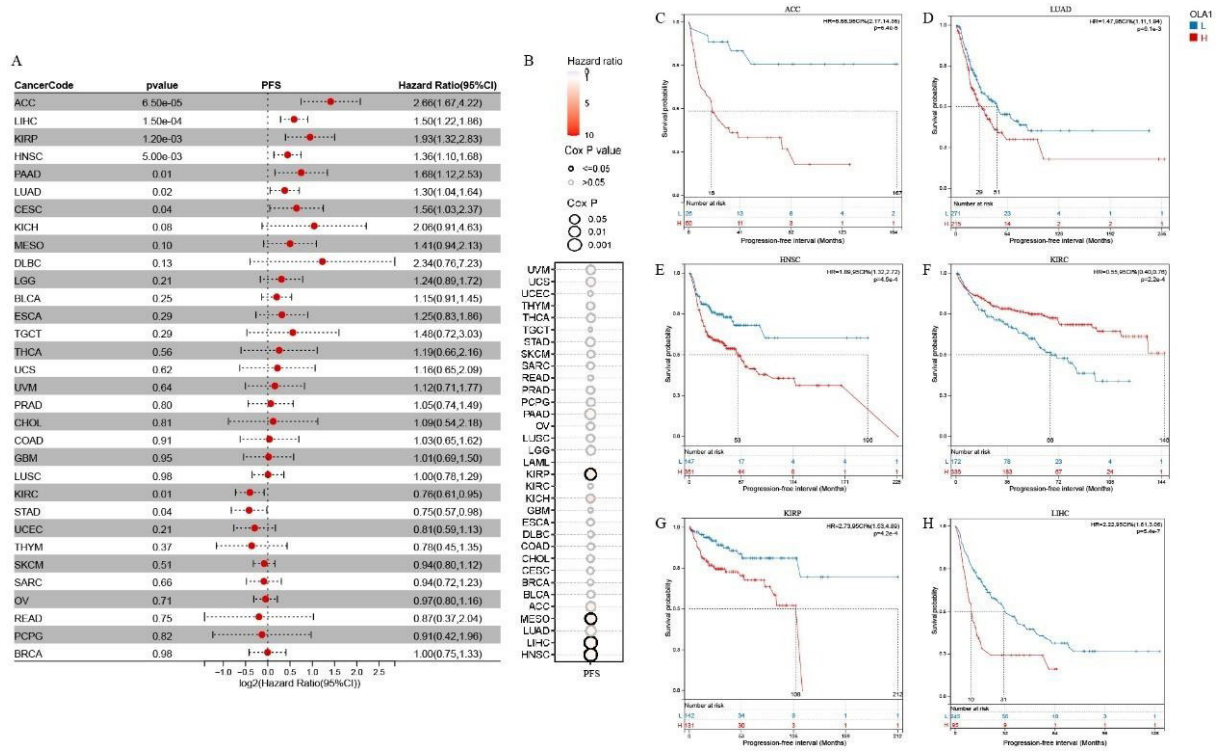

Figure 4: Correlation between Obg-like ATPase 1 (*OLA1*) expression level and Progression-Free Survival (PFS) in The Cancer Genome Atlas (TCGA) tumors. **Note:** A) Forest map shows the univariate Cox regression results of *OLA1* for PFS in tumors from TCGA database; B) Bubble plot shows the relationship between *OLA1* Gene Set Variation Analysis (GSVA) score and PFS by performing the Cox Proportional-Hazard model; C-H) Kaplan-Meier curves shows the expression of *OLA1* in 6 TCGA tumors most significantly associated with Disease-Specific Survival (DSS) (p<0.01).

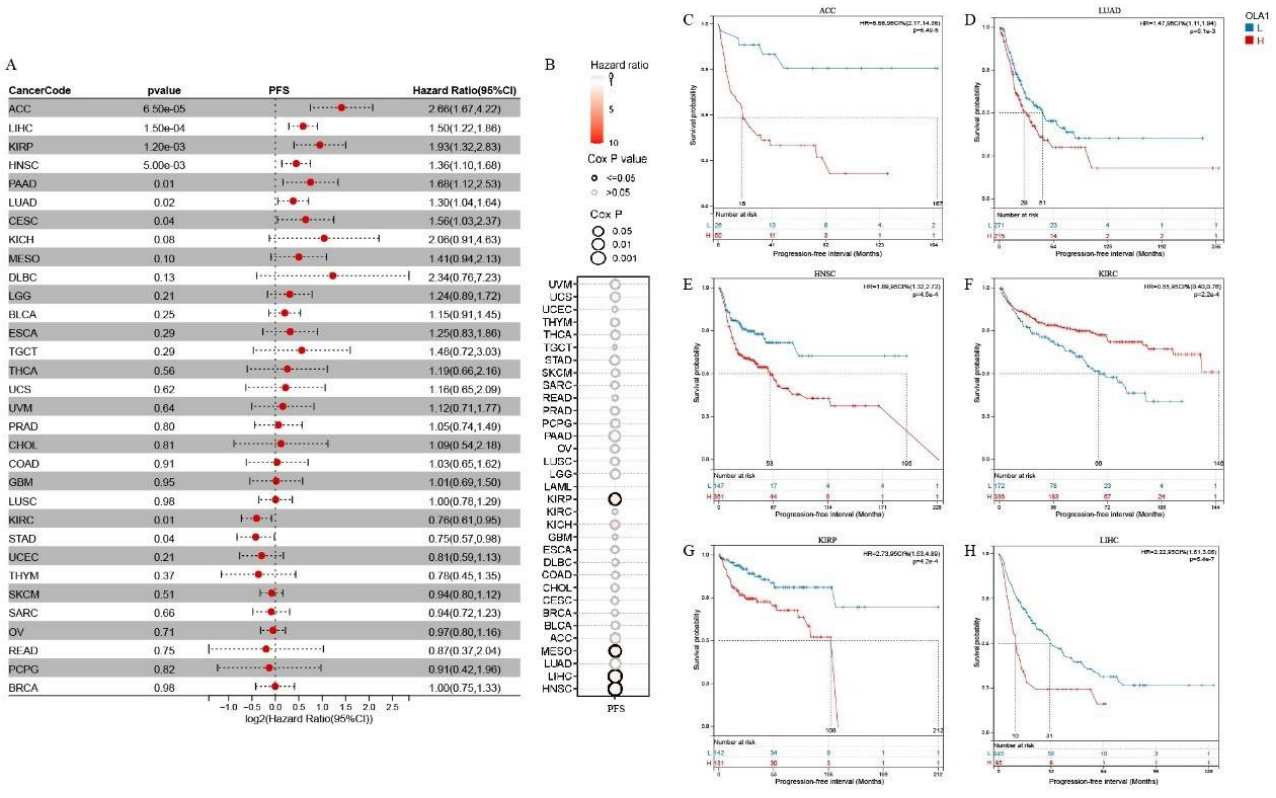

Figure 5: Correlation between Obg-like ATPase 1 (*OLA1*) expression level and Disease Free Interval (DFI) in The Cancer Genome Atlas Program (TCGA) tumors. **Note:** A) Forest map shows the univariate Cox regression results of *OLA1* for DFI in tumors from TCGA database; B) Bubble plot shows the relationship between *OLA1* Gene Set Variation Analysis (GSVA) score and DFI by performing the Cox Proportional-Hazard model; C-H) Kaplan-Meier curves shows the expression of *OLA1* in 6 TCGA tumors most significantly associated with DFI (p<0.05).

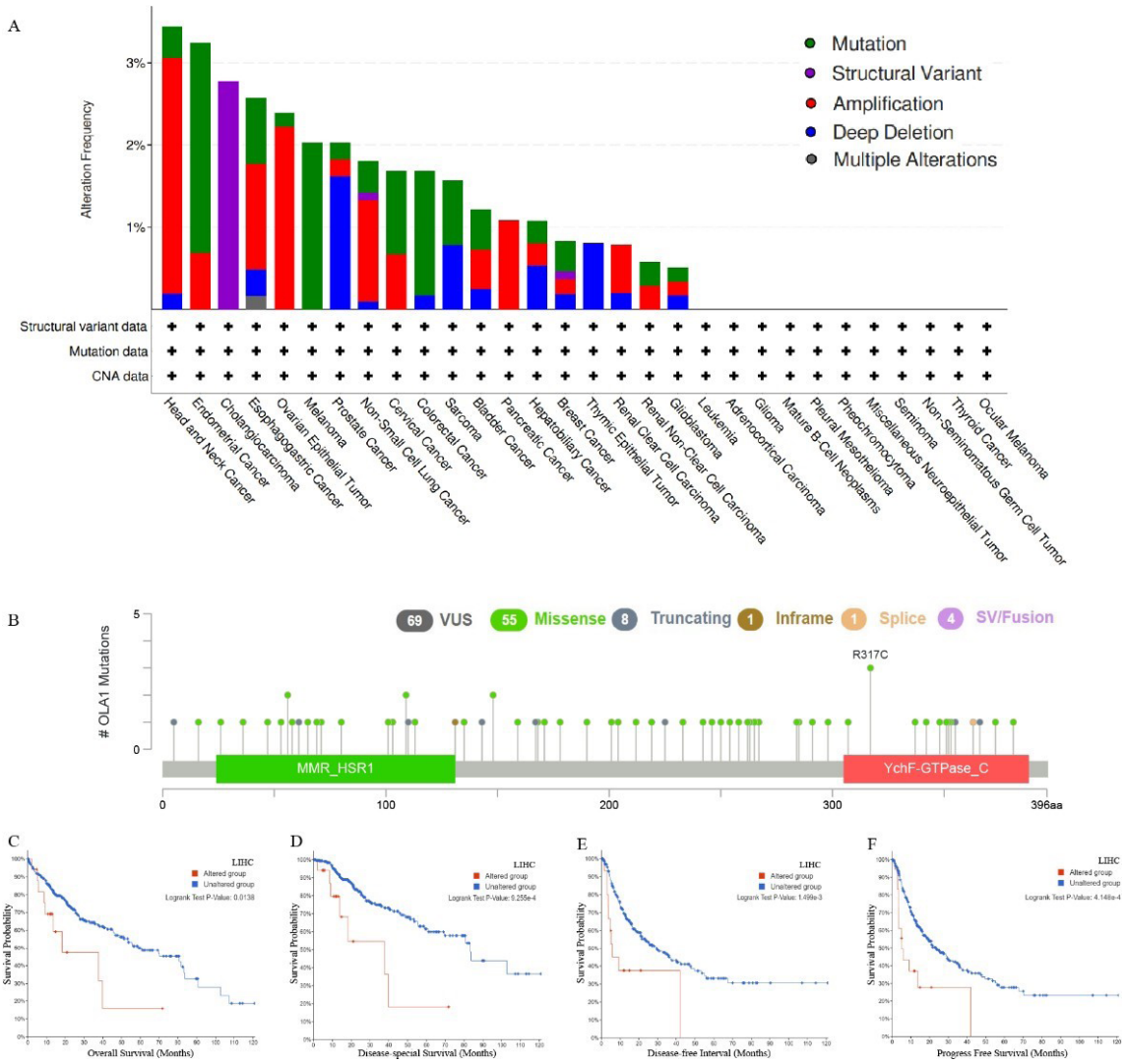

Figure 6: Obg-like ATPase 1 (*OLA1*) mutation status and survival analysis in The Cancer Genome Atlas Program (TCGA) tumors by cBioPortal website. **Note:** A) The frequency with alteration type of *OLA1* was shown ordered by cancer type across all TCGA tumors. The alteration type including mutation, structural variant, amplification, deep deletion and multiple alterations; B) The frequency with mutation site of *OLA1* was displayed and the most frequent mutation site was R317C; (C) Survival analysis of the correlation between *OLA1* mutation status Overall Survival (OS); D) Disease-specific survival (DSS); E) Disease Free Interval (DFI); (F) Progression Free Survival (PFS) of Liver Hepatocellular Carcinoma (LIHC).

OLA1 expression related with TMB, MSI, CNV and DNA methylation

TMB, MSI, CNV and DNA methylation were considered essential matters which had influence on tumorigenesis and development. At first, we investigated the relationship between *OLA1* expression and TMB or MSI in 35 cancer types. TMB, a prospective quantitative genomic biomarker for immunotherapy response irrespective of MSI or Programmed Death-Ligand 1 (PD-L1) expression status, quantifies the total number of mutations present in a tumor specimen. Based on TMB data, Spearman analysis results showed increased *OLA1* expression was considerably related with elevated TMB in LGG, LUAD, LAML, STAD, PRAD, HNSC, LUSC, THYM, MESO, PAAD, Tenosynovial Giant Cell Tumor (TGCT) and ACC, while, in KIRP and THCA, increased *OLA1* expression linked with decreased TMB (Figure 7A, $p<0.05$). MSI results from Mismatch Repair (MMR) deficiency are associated with patient outcomes [36,37]. Depending on data of MSI, our results demonstrated that significant correlations between increased *OLA1* expression levels and improved MSI were found in tumors including CESC, STAD and MESO. Conversely, *OLA1* expressions were negatively associated with MSI in LGG, LUAD, COAD, *BRCA*, PRAD, Thyroid Carcinoma (THCA) and DLBC (Figure 7B, $p<0.05$).

Next, we analyzed the relationship between CNV and *OLA1* mRNA expression through Spearman analysis across 33 cancers using GSCA platform. The coherent results indicated that *OLA1* expressions had substantially positive correlations with CNV in 22 of 33 cancers (Figure 7C, FDR ≤ 0.05), with the exception of LAML, MESO, LGG, UVM, KIRP, PCPG, THYM, THCA, GBM, DLBC and CHOL (Figure 7C, FDR>0.05).

Further, *OLA1* DNA methylation profile in 33 cancers was also detected by GSCA. *OLA1* methylation was shown to be strongly correlated with *OLA1* expression in several cancers. In MESO, GBM, LUAD, *BRCA*, LUSC, PCPG, THYM and THCA, increased *OLA1* expression levels were linked with decreased *OLA1* methylation levels, while the opposite correlations were found in PRAD, KIRC and LGG (Figure 7D, FDR ≤ 0.05) (Figure 7A-7D).

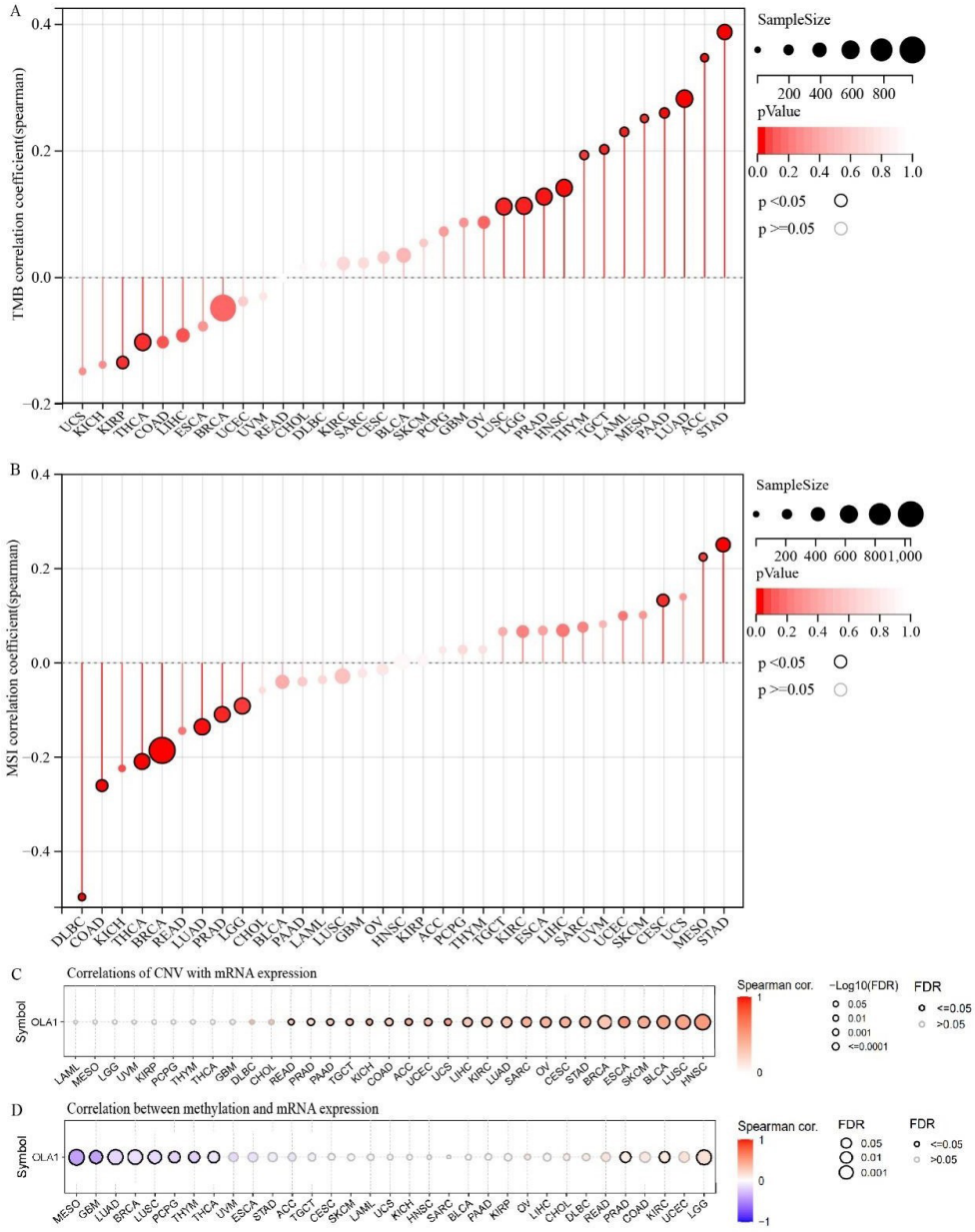

Figure 7: Correlation of Obg-like ATPase 1 (*OLA1*) expression with genetic alterations in The Cancer Genome Atlas Program (TCGA) tumors. **Note:** A) Tumor Mutational Burden (TMB); B) Microsatellite Instability (MSI); C) Copy Number Variation (CNV) and D) Deoxyribonucleic Acid (DNA) methylation. Spearman correlation test, p<0.05/False Discovery Rate (FDR) ≤ 0.05 was considered significant according to different indicators.

CNV and methylation of *OLA1* correlated with prognosis

As our results above, CNV and methylation of *OLA1* were correlated with *OLA1* expression in multiple cancer types. We further explored if *OLA1* CNV gene set CNV or methylation had significant connection with OS, DSS, DFI and PFS on GSVA website. Our results showed *OLA1* CNV levels were significantly correlated with OS in ACC, SARC and UCEC, with DSS in ACC, SARC, UCEC and STAD, with DFI in UCEC, COAD, DLBC and TGCT, with PFS in ACC, SARC, UCEC, PRAD, SKCM, TGCT and THCA (Figure 8A, p<0.05). Similarly, *OLA1* gene set CNV which represented integrated CNV level of *OLA1* had noticeably connections with OS among patients with ACC, SARC and UCEC, with DSS in ACC, SARC, UCEC and STAD, with DFI in UCEC, COAD, DLBC and TGCT, with PFS in ACC, SARC, UCEC, PRAD and TGCT patients (Figure 8B, p<0.05).

Moreover, the results between *OLA1* methylation and prognosis indicated that lower *OLA1* methylation was associated with poor OS in KIRC (HR=0.59, p<0.01), while in THCA (HR=3.19, p<0.05), lower *OLA1* methylation linked with a longer OS. Of DSS results, only in KIRC (HR=0.59, p<0.05), *OLA1* methylation had a negative correlation with DSS there were no significant results in other cancers. In HNSC (HR=1.39, p<0.01), higher *OLA1* methylation level was associated with a shorter PFS, however, it associated with longer PFS in PRAD (HR=0.62, p<0.05) and BLCA (HR=0.75, p<0.05). No correlation was found between *OLA1* methylation level and DFI in any cancer types (Figure 8C, p>0.05) (Figures 8A-8C).

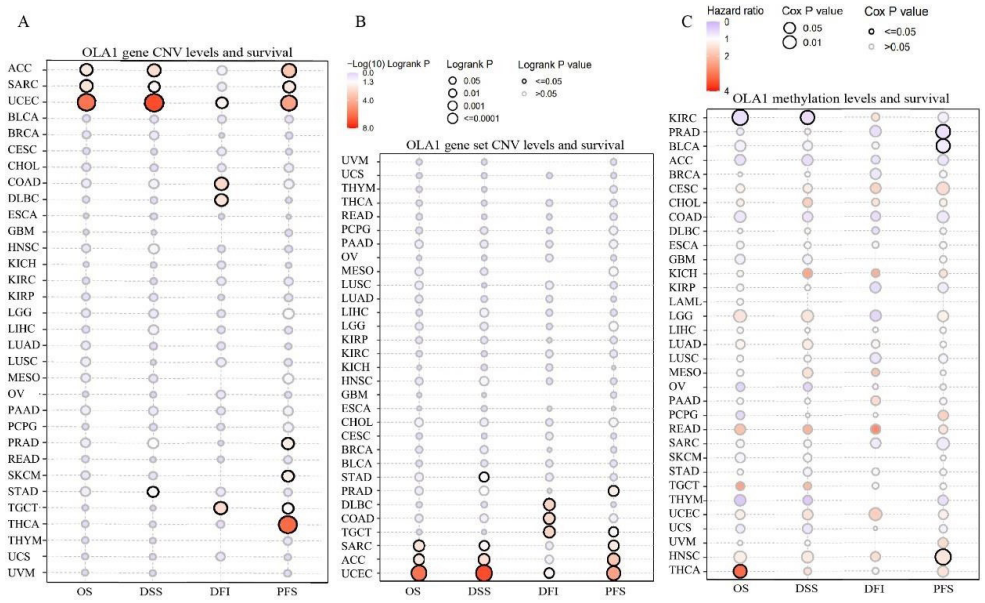

Figure 8: Obg-like ATPase 1 (*OLA1*) Copy Number Variation (CNV) and methylation levels correlated with survival in pan-cancer using Gene Set Cancer Analysis (GSCA) tool. Correlation between. **Note:** A) *OLA1* gene; B) Gene set CNV level and Overall Survival (OS), Disease-specific Survival (DSS), Disease Free Interval (DFI), Progression-Free Survival (PFS). Logrank p ≤ 0.05 was as significant; C) The relationship between *OLA1* methylation and survival types, including OS, DSS, DFI, PFS. Cox p ≤ 0.05 was as significant.

OLA1 expression linked with immune infiltration in cancers

To clarify the role of *OLA1* in the TME, TIMER2.0 tool was applied for analyzing the association between *OLA1* expression and the infiltrations of CAFs, macrophages and endothelial cells. We acquired a consistent result that *OLA1* expression was negatively associated with CAF in COAD, LUSC, OV, SARC and STAD by EPIC, MCP-counter, XCELL, TIDE algorithms (Figure 9A, p<0.05). In CESC, COAD, GBM, LGG, LUSC, OV, SARC, UCEC and UCS, *OLA1* expression levels were negatively related with macrophage infiltrations through EPIC, TIMER, XCELL algorithms. Also, a unanimous result showed that *OLA1* expression was negatively linked with endothelial cells in BLCA, *BRCA*-Basal, COAD, LUAD, LUSC, PCPG and STAD by EPIC, MCP-counter and XCELL algorithms. Combined with three results above, we found *OLA1* expressions were negatively correlated with immune infiltrations of CAFs, macrophages and endothelial cells only in two cancer types, COAD and LUSC. We chose COAD to exhibit the comprehensive results of the correlation between *OLA1* expression and immune infiltrations using different algorithms by performing the scatterplots (Figures 9C-9L, p<0.05). Moreover, we detected the GSVA score of *OLA1* correlation with 24 immune cells infiltration from ImmuCellAI based on GSCA platform, which including 18 T-cell subtypes and 6 other immune cells: B cell, Natural Killer (NK) cell, monocyte cell, macrophage, neutrophil and Dendritic cell (DC). We observed that *OLA1* GSVA score had significantly negative relationship with monocyte cell infiltration in LGG, PCPG, KIRP and GBM, but had opposite connection in SKCM, PRAD and THCA (FDR ≤ 0.05). All results were shown in a heatmap (Figures 9A-9L).

We further calculated the immune, stromal and estimate scores for each tumor sample from TCGA and GTEx databases. The top 3 tumors with the most significant relationships between *OLA1* expression and the TME were SARC, LUSC and STAD (stromal score), LUSC, LGG and THCA (immune score), LUSC, LGG and THCA (estimate score) respectively (Figure 10, p<0.001). The three types of scores of other cancers were performed (Figures 10A-10C).

Finally, we investigated the relationships between *OLA1* expression and different tumor immune subtypes based on TISIDB website. The results proved that *OLA1* expression was significantly correlated with immune subtypes including C1: Wound healing, C2: IFN-gamma dominant, C3: Inflammatory, C4: Lymphocyte depleted, C5: Immunologically quiet and C6: TGF-beta dominant of BLCA, *BRCA*, COAD, ESCA, KIRC, KIRP, LIHC, LUAD, LUSC, MESO, PCPG, PRAD, READ, STAD, UCEC and UVM, while in other tumors, we were failure to carry out the differences between *OLA1* and immune subtypes.

Correlation of *OLA1* with immunoregulation-related genes and immune checkpoints

To further study the relationship between *OLA1* and immune aspects, we conducted a Spearman analysis to explore co-expression of immunoregulation-related genes in pan-cancer. The immunoregulation-related genes mainly consist of chemokines, chemokine receptors, Major Histocompatibility Complex (MHC), immune-inhibitor and immune-stimulator genes. The results from chemokines and chemokine receptors data illustrated that the majority immune-related genes were positively associated with *OLA1* in cancer types, except for KICH, ESCA, LUSC, LUAD, STAD, COAD and SARC (p<0.05). As for MHC data, most of immune-related genes were substantially negative correlated with *OLA1*, however, there were converse results in LIHC, DLBC, KIRC and PCPG (p<0.05). Next, we focused on data of immune-inhibitor and immune-stimulator genes. Our results indicated that *OLA1* had negative connection with immune-related genes expression mainly in KICH, ESCA, LUSC, LUAD, STAD, COAD and SARC, but had positive correlations mainly with LIHC, KIRC, KIRP, PRAD, UCEC and BLCA (p<0.05). It was worth noting that

OLA1 expression had similar relationship with immunoregulation-related genes in cancer types as follows: KICH, ESCA, LUSC, LUAD, STAD, COAD, LIHC and KIRC (Figure 11).

Moreover, 60 immune checkpoint genes were selected for analyzing the correlation between *OLA1* expression and immune checkpoint gene expression, which results were displayed in a heatmap. In a variety of cancers such as KICH, BLCA, KIRP, PAAD, SKCM, UCEC, PRAD and KIRC, *OLA1* expression was positively associated with the expression levels of the mostly immune checkpoint genes ($p<0.05$). On the contrary, in LIHC, ESCA, LUAD and COAD, the results showed negatively connections between *OLA1* expression and immune checkpoint gene expressions (Figure 12, $p<0.05$).

Immunotherapy and drug response of *OLA1*

To investigate the promising value of *OLA1* as an innovative immune target in pan-cancer, we anticipated the immunotherapy and sensitive medicines based on *OLA1* (Figure 12). TISMO was used to evaluate the immunotherapy response of *OLA1*. TISMO is a database specifically designed for hosting, visualizing and analyzing an extensive collection of syngeneic mouse model data [31]. On the TISMO website, tumor models were including as follows: Mammary cancer: 4T1, E0771, EMT6, T11, KPB25L, p53-2225L, p53-2336R; Colorectal carcinoma: CT26, MC38; Gastric adenocarcinoma: YTN16; Head and neck squamous cell carcinoma: MOC22; Hepatocellular carcinoma: BNL-MEA; Lung carcinoma: LLC; Melanoma: B16, YUMM1.7, D3UV2, D4M.3A.3; Sarcoma: 402230. Anti-PDL1, Anti-PDL2 and Anti-CTLA4, 4 immune treatments, were used to analyze. Our results indicated that *OLA1* could predict immunotherapy response in 5 murine immunotherapy cohorts. Non-responders were more likely to have increased *OLA1* levels in 3 cohorts of 4T1 and T11 in mammary cancer (FDR ≤ 0.05). In "EMT6_GSE107801_Anti-PDL1" cohort, responders were significantly correlated with high levels of *OLA1* (FDR ≤ 0.001), however, responders had notable connections with decreased levels of *OLA1* in "YTN16-GSE146027-day21-AntiCTLA-4" cohort (Figure 12A, FDR ≤ 0.001).

Furthermore, we predicted the sensitive drugs of *OLA1* based on CTRP and GDSC databases using GSCA tool. The relationship between *OLA1* expression levels and drug sensitivity based on CTRP dataset indicated that BI-2536 (Serine/threonine-protein kinase PLK1 inhibitor), ciclopirox (CPX) and GSK461364 (ATP-competitive inhibitor of PLK1) were the top 3 drugs which negatively linked with *OLA1* expression levels (Figure 12B, FDR ≤ 0.001). The correlation between *OLA1* levels and drug sensitivity based on GDSC dataset showed that FK886 (targeted Nicotinamide phosphoribosyltransferase (NAMPT) inhibitor), NPK76-II-72-1 (targeted Mammalian Polo-like kinase 3 (PLK3) inhibitor) and CX-5461 (hyperactivation of RNA polymerase I transcription inhibitor) were the top 3 drugs that negatively related to *OLA1* levels, while Z-LLNle-CHO (gamma-Secretase Inhibitor I), TGX221 (inhibitor of the PI3K p110β catalytic subunit) and Bortezomib (26S proteosome inhibitor) were the top 3 drugs that positively linked with *OLA1* expressions (Figure 12C, FDR ≤ 0.001) (Figures 12A-12C).

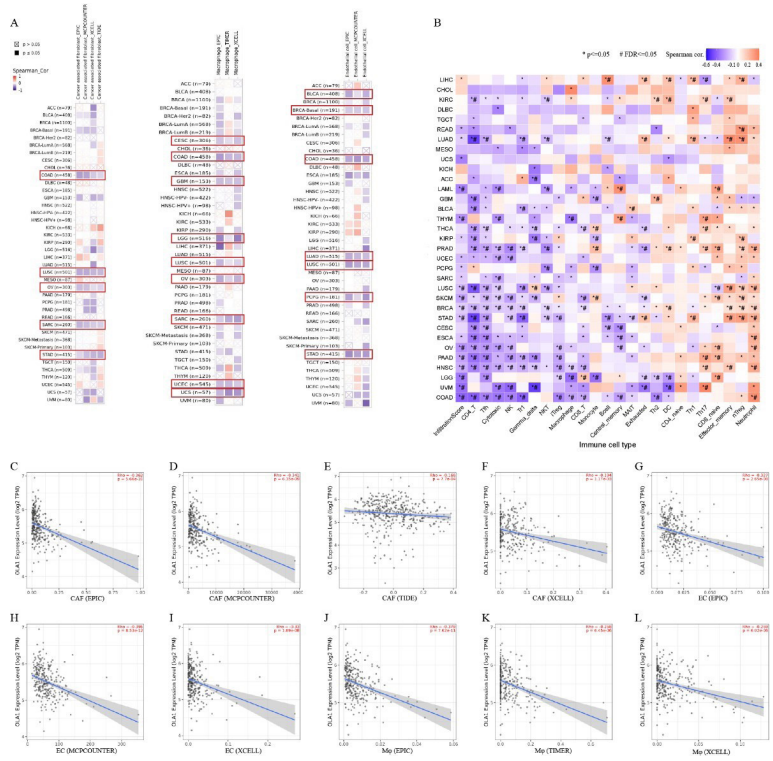

Figure 9: Correlation with Obg-like ATPase 1 (*OLA1*) expression and immune cell infiltration. **Note:** A) Tumor IMmune Estimation Resource (TIMER), epic, tide, xcell and mcpcounter algorithms were used for the spearman correlation analysis of the level of cancer-associated infiltration of fibroblasts, macrophages and endothelial cells and the expression levels of the *OLA1* across all TCGA tumors based on TIMER2.0; B) A heatmap showed the spearman correlation analysis between Gene Set Variation Analysis (GSVA) score of *OLA1* and 24 immune cells infiltration from ImmuCellAI based on GSCA, which including 18 T-cell subtypes and 6 other immune cells: B cell, NK cell, monocyte cell, macrophage, neutrophil and Dendtric Cells (DC), p ≤ 0.05, False Discovery Rate (FDR) ≤ 0.05; C-F) Correlation with *OLA1* expression and Cancer-Associated Fibroblasts (CAF) in Colon Cancer (COAD); G-I) Correlation with *OLA1* expression and Endothelial Cells (EC) in COAD; J-L) Correlation with *OLA1* expression and Mφ in COAD.

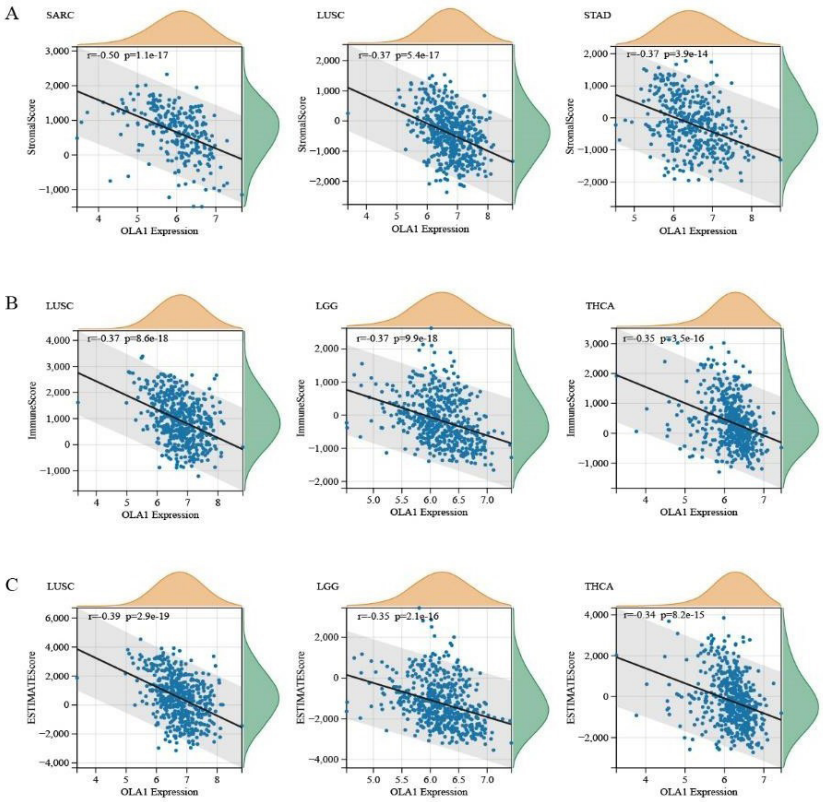

Figure 10: The top 3 tumors with the most significant relationships between Obg-like ATPase 1 (*OLA1*) expression and the tumor microenvironment according to stromal score, immune score and estimate score based on The Cancer Genome Atlas Program (TCGA) and Genotype-Tissue Expression (GTEx) databases. **Note:** A) The relationship between *OLA1* expression and stromal score in Sarcoma (SARC), Lung Squamous Cell Carcinoma (LUSC), Stomach Adenocarcinoma (STAD); B) The relationship between *OLA1* expression and immune score in LUSC, Lower Grade Glioma (LGG), Thyroid Carcinoma (THCA); C) The relationship between *OLA1* expression and estimate score in LUSC, LGG, THCA.

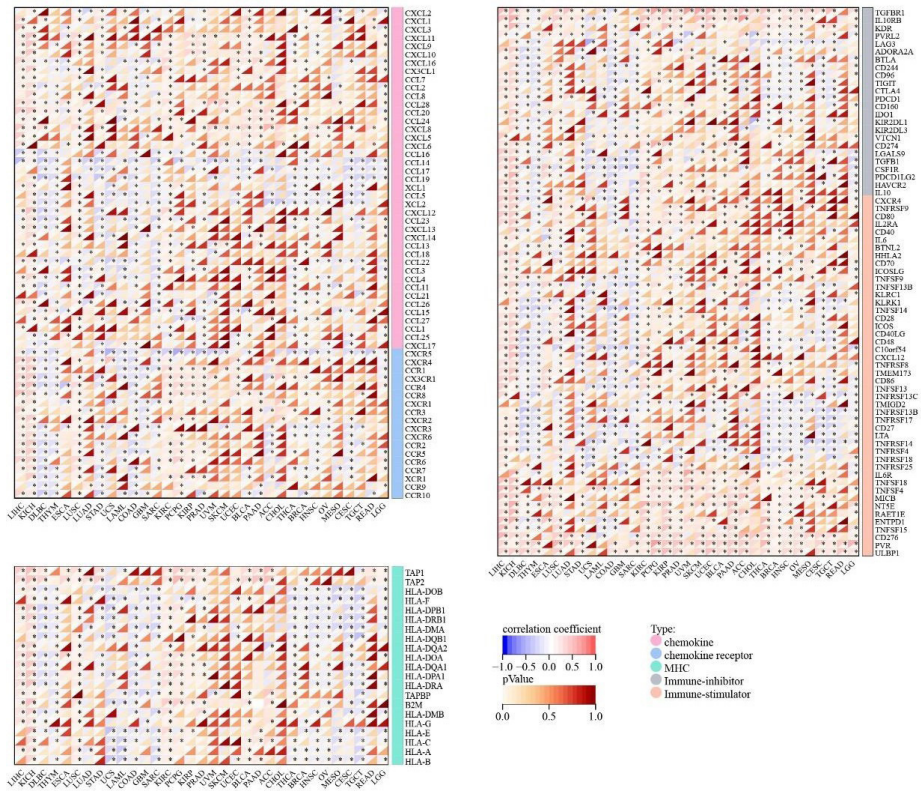

Figure 11: Co-expression of Obg-like ATPase 1 (*OLA1*) and immunoregulation-related genes in pan-cancer.

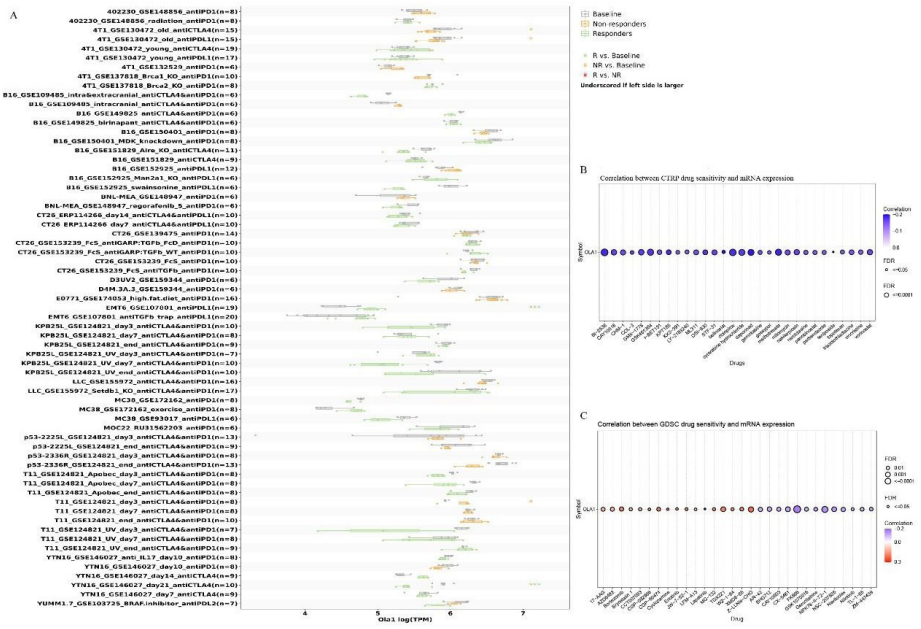

Figure 12: Immunotherapy response and drug sensitivity of Obg-like ATPase 1 (*OLA1*) in pan-cancer. **Note:** A) *OLA1* immunotherapy response analysis from Tumor Immune Syngeneic Mouse (TISMO). False Discovery Rate (FDR) ≤ 0.05, FDR ≤ 0.01, FDR ≤ 0.001. Predictive drugs based on *OLA1* expression in pan-cancer from the Genomics of Therapeutics Response Portal (CTRP); B) And GDSC; C) Datasets based on Gene Set Cancer Analysis (GSCA) (top 30 drugs).

Co-expression networks of *OLA1* and enrichment analyses in pan-cancer

In order to explore the co-expression network and enrichment pathways of *OLA1* in pan-cancer, at the RNA level, firstly, we performed correlation analysis between *OLA1* and other genes based on TCGA databases by using GEPIA2 tool. The 100 genes most positively correlated with *OLA1* were obtained for enrichment analysis and the top 50 genes were shown in a heatmap (Figure 13A). We could observe that zinc finger CCCH-type containing 15 (ZC3H15), Protein Kinase RNA-Activated (PKR)-Associated Protein (PRKRA), Single-Strand Binding protein (SSB), Methylthioadenosine Phosphorylase (*MMADHC*), *OLA1P1* and Mitochondrial Ribosomal Protein L30 (*MRPL30*) were the most positively *OLA1*-related genes (Figures 13B-13G, p<0.001) (Figures 13A-13G).

Further, the top 100 genes positively linked with *OLA1* were used for GO functional enrichment and KEGG pathway analysis to uncover the potential functional pathways. GO analysis contained three parts, Biological Process (BP), Cellular Component (CC) and Molecular Function (MF), which revealed that *OLA1* was significantly associated with RNA splicing, nucleic acid transport, DNA combination, nuclear chromatin, chromosomal region, condensed chromosome kinetochore, heat shock protein binding, single- stranded DNA binding, DNA replication origin binding and others. Similarly, the KEGG results showed that *OLA1* was involved in tumorigenesis through spliceosome, RNA transport, cell cycle and ribosome biogenesis in eukaryotes. Next, at the protein level, we exploited the GeneMANIA website to establish a PPI network for *OLA1*, which demonstrated that *OLA1* had significantly interactions with Glutamyl-prolyl-tRNA synthetase (EPRS10, Adenine Phosphoribosyltransferase (APRT), Exosome Component 3 (EXOSC3), Sorting Nexin 8 (SNF8), Guanine nucleotide-binding protein-like 3 (GNL3L) and others. Meanwhile, we predicted the *OLA1* binding proteins by STRING website, which were validated by experiment. According to our parameters setting above, there were 8 proteins including *BRAD1*, Breast Cancer-Associated Gene 1 (*BRCA1*), Tubulin Gamma 1 (TUBG1), Methionine Adenosyltransferase 1A (MAT1A), Methionine Adenosyltransferase 2A (MAT2A), B-Cell Receptor-Associated Protein 31 (BCAP31), Prohibitin (PHB) and Heat Shock Protein Family A (Hsp70) Member 9 (*HSPA9*) binding to *OLA1* (Figures 14A-14C).

OLA1 protein expression level correlated with cancer-related pathway activity

Next, GSCA platform was used to evaluated the connection between *OLA1* protein expression level and pathway activity activation and inhibition groups in pan-cancer based on The Cancer Proteome Atlas (TCPA) and TCGA databases. On GSVA website, the pathways mainly associated with tumor proliferation, such as TSC/mTOR, Receptor Tyrosine Kinases (RTK), RAS-Mitogen-Activated Protein Kinase (RASMAPK), PI3K/AKT, Hormone Estrogen Receptor (ER), Hormone Androgen Receptor (AR), Epithelial-Mesenchymal Transition (EMT), DNA damage response, cell cycle and apoptosis and the pathway activity was defined by median Pathway Score (PAS). From the results, we found that *OLA1* mainly had effects on pathways as follows, cell cycle activation (28% cancer types), RASMAPK inhibition (19%), apoptosis activation (16%), DNA damage activation (16%) and others (Figure 15A). In detail, high *OLA1* expression might have active effects on cell cycle pathway in *BRCA*, COAD, ESCA, KIRP, LUAD, LUSC, STAD, TGCT and THYM (Figures 15C-15K, FDR ≤ 0.05). On the contrary, in *BRCA*, LIHC, LUAD, LUSC, LGG and THYM, high *OLA1* expression levels had potential inhibitive effects on RASMAPK pathway (Figures 15L-15Q, FDR ≤ 0.05). Meanwhile, we also estimated the relationship between *OLA1* GSVA score and pathway activity, which results showed that *OLA1* GSVA score was mainly associated with cell cycle (31%), DNA damage (28%), RTK (25%), PI3K/AKT (22%) and RASMAPK (22%) pathways. For

example, high *OLA1* GSVA score indicated the active effects on cell cycle pathway in cancers including COAD, ESCA, HNSC, KIRP, LUAD, LUSC, SKCM, STAD, TGCT and THYM. Interestingly, high *OLA1* GSVA score might have inhibitive effects on RAS/MAPK pathway among patients with COAD, LGG, LIHC, LUAD, LUSC and THYM, but it had an activate function in KICH (Figure 15B, FDR ≤ 0.05) (Figures 15A-15Q).

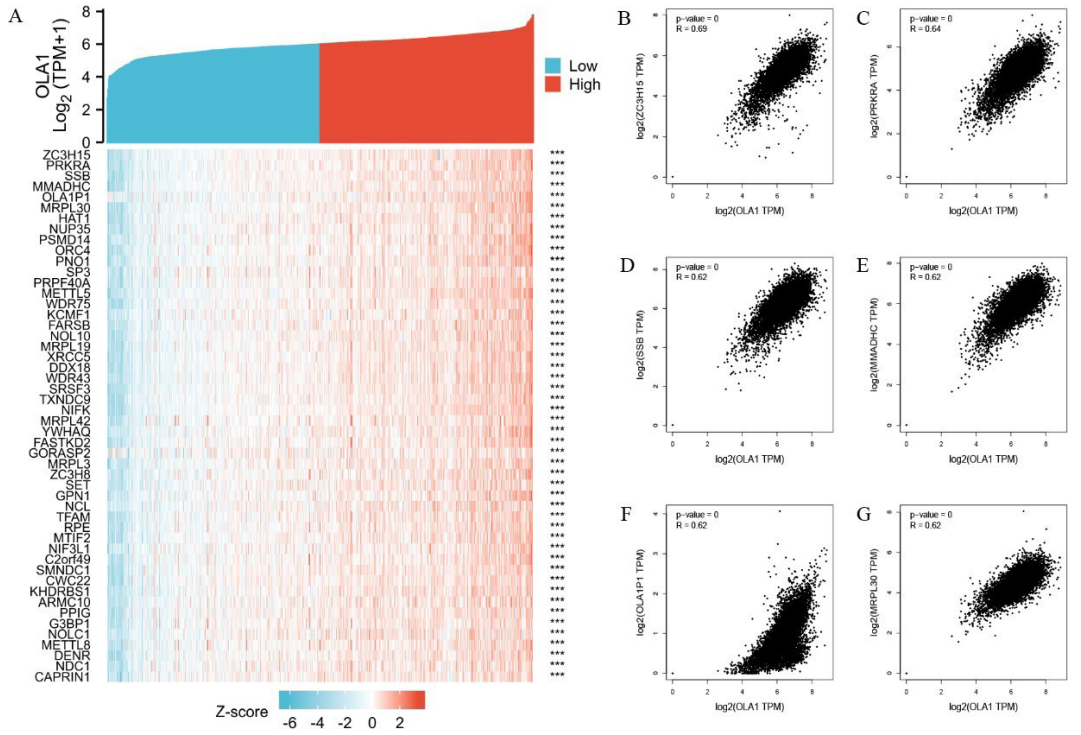

Figure 13: The correlation analysis of Obg-like ATPase 1 (*OLA1*) in pan-cancer based on the The Cancer Genome Atlas Program (TCGA) tumor and normal databases by using GEPIA2 tool. **Note:** A) The top 50 genes most positively associated with *OLA1* which collected from Gene Expression Profiling Interactive Analysis (GEPIA2) similar genes detection module were shown in a heatmap. The six highest positively correlation genes with *OLA1* expression were displayed separately by GEPIA2 correlation analysis module, which were; B) Zinc finger CCCH-type containing 15 (ZC3H15); C) Protein Kinase RNA-Activated (PKR)-Associated Protein (PRKRA); D) Single-Strand Binding Protein (SSB); E) Methylmalonic Acidemia with Homocystinuria (*MMADHC*); F) *OLA1P1* and; G) Mitochondrial Ribosomal Protein L30 (*MRPL30*) shown in scatterplots.

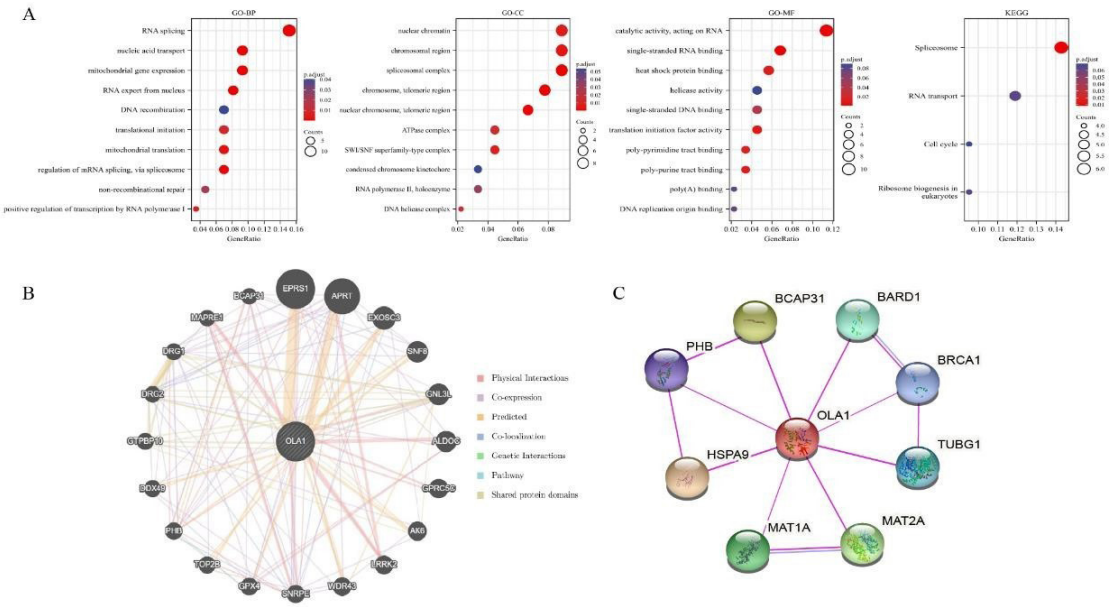

Figure 14: Co-expression network of Obg-like ATPase 1 (*OLA1*) and enrichment analysis in pan-cancer. **Note:** A) Significant Gene Ontology (GO) terms of top 100 genes most positively correlated with *OLA1*, including Biological Process (BP), Cellular Component (CC), Molecular Function (MF) and the result of Kyoto Encyclopedia of Genes and Genomes (KEGG) pathway analysis; B) A Protein-Protein Interaction (PPI) network of *OLA1* from Gene Multiple Association Network Integration Algorithm (GeneMANIA) website; C) Search Tool for the Retrieval of Interacting Genes/Proteins (STRING) protein network map of experimentally determined *OLA1*-binding proteins.

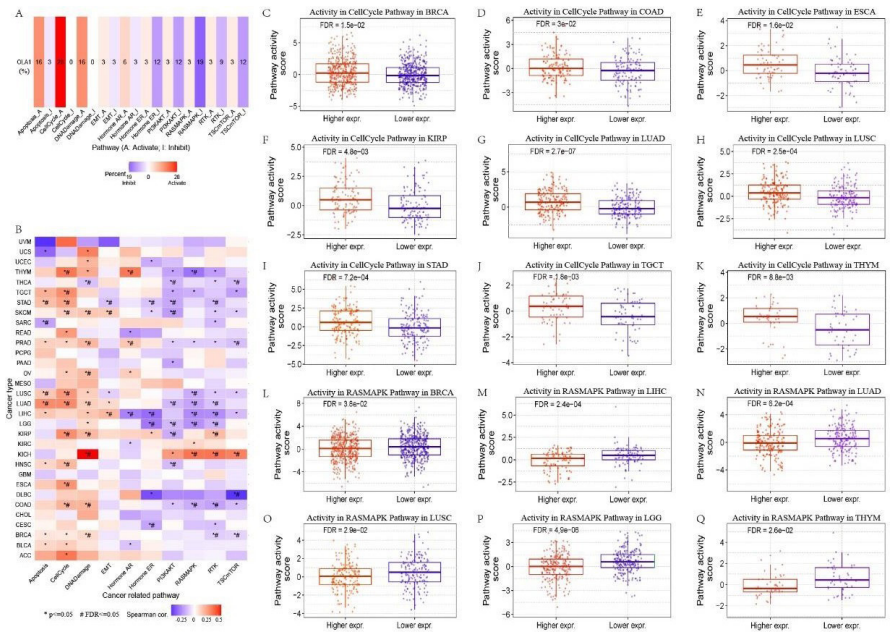

Figure 15: Obg-like ATPase 1 (*OLA1*) correlation with pathway activity from Gene Set Cancer Analysis (GSCA) platform. **Note:** A) The relationship between *OLA1* expression and pathway activity activation and inhibition groups; B) The relationship between *OLA1* Gene Set Variation Analysis (GSVA) score and pathway activity, $p \leq 0.05$, False Discovery Rate (FDR) ≤ 0.05. The number in each cell indicated that the percentage of 32 cancer types, in which *OLA1* expression showed significant association with a specific pathway (FDR ≤ 0.05). The percentages above 18% tumors were shown in the box plots. 28% tumors may have an activation effect on cell cycle pathway, including; C) BReast CAncer gene (*BRCA*); D) Colon Cancer (COAD); E) Esophageal Cancer (ESCA); F) Kidney Renal Papillary cell carcinoma (KIRP); G) Lung Adenocarcinoma (LUAD); H) Lung Squamous Cell Carcinoma (LUSC); I) STAD; J) TGCT; K) Thymoma (THYM). 19% tumors may have an inhibition effect on RAS-Mitogen-Activated Protein Kinase (RASMAPK) pathway, including; L) *BRCA*; M) LIHC; N) LUAD; O) LUSC; P) LGG; Q) THYM.

DISCUSSION

OLA1 is widely present in the cytoplasm and is expressed in a variety of tissues. As previously mentioned, *OLA1* is highly conserved from bacteria to human, pointing to its important functions in fundamental cellular processes and intracellular homeostasis. Our study indicated that *OLA1* expression was generally higher in tumor tissues than normal controls in 26 types of malignancies and the similar results were confirmed at protein levels from HPA. Previous studies showed that increased *OLA1* expressions were found in UCEC, LUSC, LUAD, LIHC, COAD tumor tissues than those in normal tissues, which were consistent with our results. However, Liu et al. demonstrated that *OLA1* expression was lower in tumor tissues in oral squamous cell carcinoma and might promote EMT and metastasis, which contradicted our results [11,12]. The discrepancy is probably due to more samples were analyzed in TCGA database besides the patients with oral squamous cell carcinoma. Interestingly, *OLA1* is lower expressed in tumor tissues than those in normal controls in KICH [38-40].

Moreover, our Cox regression and Kaplan-Meier analyses using the TCGA databases suggested an association between high expression of *OLA1* and poor prognosis in LUAD, LIHC, ACC, CESC, PAAD. Similarly, it was reported that increased expression of *OLA1* was substantially linked with shorter OS in lung cancer and hepatocellular carcinoma patients [12,39]. Our prior report demonstrated that increased expression of *OLA1*, an independent risk factor, was linked with poor OS in patients with COAD and READ, yet we failed to detect the survival difference in this study probably due to the race and sample size [40]. In contrast, upgraded *OLA1* expression was associated with an opposite prognosis in patients with KIRC, STAD and OV. Therefore, it is reasonable that *OLA1* may serve different functions in different tumors and could be a prognostic biomarker in pan-cancer. In addition, we observed that *OLA1* expression was related to the pathological stages in some cancers. *OLA1* expression was higher in advanced stage in patients with LIHC and LUAD, which was in line with prior results. Further, *OLA1* expression varied in different molecular subtypes in a few types of cancers. These results suggested *OLA1* might be an important player in guiding the choice of anti-cancer therapy in patients with different pathological stages and molecular subtypes in the era of precision medicine.

Genomic instability, especially some specific genetic and epigenetic changes, is a feature of cancer which results in defective apoptosis. Consequently, we also concentrated on CNV, DNA methylation, TMB and MSI of *OLA1*. CNV is a type of genomic structural variation that causes abnormal or normal variation in the number of copies of one or more sections of some specific genes, including protein-coding and non-protein-coding genes. The larger CNVs (more than 250 kb) were considered to be associated with morbid consequences such as developmental disorders and cancers [41-44]. Graf et al., validated that CNV was an independent risk factor in OV cancer patients. In this study, we also discovered a positive correlation between CNV and OLA expression in 22 types of malignancies and a negative relationship of prognosis in ACC, SACR and UCEC. DNA methylation is one of the most studied epigenetic modifications in mammals, which ensures optimal gene expression regulation and long-term gene silencing [45]. It was reported that abnormal DNA methylation levels could lead to the inactivation of tumor suppressors resulting in promoting tumor genesis in multiple cancers. Our results carried out that higher *OLA1* methylation was related to shorter OS in THCA and longer OS in KIRC. It is plausible to reason that *OLA1* methylation has complicated roles in different cancers, which needs more clinical data and experiments to verify. Hence, aberrant *OLA1* expression

may exert impact on tumor progression partially through influence on mechanisms that maintaining genomic stability [46,47].

TMB is regarded as an emerging biomarker for response to Immune-Checkpoint Inhibitors (ICIs) recently. It is believed that increased TMB prompts more tumor neoantigens, leading to more opportunities for T cells recognition and correlates with better immunotherapy outcomes in clinical practices. In addition to TMB, MSI represents another extensively studied marker that was a part of genomic instability and might predict response to ICIs. It was demonstrated that functional loss mutations in mismatch repair pathway genes correlated with TMB-high (TMB-H) in tumors and unsurprisingly MSI-high (MSI-H) generally occurred as a subset of TMB-H. Nevertheless, the converse was not true, which meant there were plenty of patients who presented TMB-H but showed Microsatellite-Stable (MSS). Interestingly, TMB-H with MSS were more common than MSI-H in tumors and might benefit from ICIs as well. We pointed that the level of TMB was positively correlated with the expression of *OLA1* in 14 types of malignancies, while only 3 cancers showed a positive correlation trend among MSI and *OLA1* expression. Above these cancer types, STAD and MESO exhibited the same alter trend however, more cancers showed the opposite trend, such as LGG, LUAD and PRAD, which indirectly confirmed previous research that the co-occurrence of TMB-H and MSI-H was strongly dependent on the cancer types [48-52].

Based on the existing researches and our findings, *OLA1* shed new light on immunotherapy strategies. TME is made up of multiple cell types (fibroblasts, immune cells, endothelial cells, etc.) and extracellular concepts (cytokines, growth factors, hormones, extracellular matrix, etc.) that surround and feed tumor cells through vascular networks. Tumor-infiltration immune cells in TME may behave in ways that are tumor-antagonizing or tumor-promoting and have connections to clinical outcomes. Our investigation found a substantial negative correlation between *OLA1* and immune, stromal and estimate scores in most cancer types, which might have an impact on carcinogenesis [53,54].

Involved in a variety of malignant biological activities of cancer cells, such as proliferation, invasion, metastasis, immune suppression and treatment resistance, CAFs are an essential part of the TME. In general, numerous investigations showed that CAFs were critical in tumorigenesis and predicted a poor prognosis. However, other researchers demonstrated that CAFs could also limit tumor growth. It was reported that CAFs mainly consisted of heterogeneous subtypes with different functions, including myofibroblastic CAFs, inflammatory CAFs, antigen- presenting CAFs and others. In the current study, we observed that increased *OLA1* expressions were associated with decreased CAF infiltrations in COAD, LUSC, OV, SARC and STAD. Combined with our earlier study and the research above, *OLA1* may contribute to a poor prognosis through inhibiting CAFs infiltration levels in COAD, which are probably dominated by tumor suppressor components. Therefore, *OLA1* may function as an oncogene in diverse malignancies and further researcher are required to determine how *OLA1* might regulate CAFs [55-64].

Historically, tumor histological features and tissue origin were used to classify tumors. With the rise of tumor immunotherapy, it is essential to figure out if TME components may be exploited as targets for tumor immunotherapy. Recently, Thorsson et al., reported a novel method for classifying tumor immune subtypes using immunogenic analysis of 33 TCGA cancers. 6 immune subtypes were identified, which were C1 (wound healing), C2 (IFN-gamma dominant), C3 (inflammatory), C4 (lymphocyte depleted), C5 (immunologically quiet) and C6 (TGF-beta dominant). These 6 categories represent characteristics of TME that suggest certain treatment approaches may be independent of histologic types [30]. Our analysis of the immune subtypes in patients with pan-cancer revealed that *OLA1* expression was significantly abnormal in different immune subtypes among those with BLCA, *BRCA*, COAD, ESCA, KIRC, KIRP, LIHC, LUAD, LUSC, MESO, PCPG, PRAD, READ, STAD, UCEC and UVM, suggesting that *OLA1* might be a target in cancer immunotherapy.

Additionally, our study found a relationship between *OLA1* expression and genes associated to immunoregulation, including chemokines, chemokine receptors, MHC, immune-inhibitors and immune-stimulators. Finally, we detected the relationship between more than 60 immune checkpoints and *OLA1*. The majority of immune checkpoints, such as CD276, HMGB1, CTLA4 and others, were discovered to be highly related to *OLA1* levels. Our results from TISMO also manifested that *OLA1* could anticipate 5 murine immunotherapy groups. The combined results indicate that *OLA1* is closely correlated with tumor immune cell infiltrations, implying that it could be a novel biomarker for predicting immunotherapy response and prognosis.

As shown in the observations of our enrichment analyses, *OLA1* was tightly associated with cell proliferation at the transcript level, including cell cycle, DNA combination, single-stranded DNA binding, DNA replication origin binding, nuclear chromatin, chromosomal region and others. Lu et al., showed that IMP2, a reader of N6 methyladenosine, enhanced colorectal cancer cell proliferation, colony information and apoptosis inhibition through stabilizing the ZFAS1/*OLA1* axis [65]. Dong et al., reported that *OLA1* could be a potential prognostic indicator and a therapeutic target in endometrial cancer by regulating the TGF-β signaling, want signaling and ubiquitin-mediated proteolysis pathways [13]. Similar to what we previously discovered, *OLA1* increased colorectal cancer carcinogenesis by activating the HIF1α/CA9 axis. Liu et al., found that *OLA1* could suppress oral squamous cell metastasis by inhibiting the activity of a TGFβ/SMAD2/EMT pathway [11]. Combining with above studies and our analyses, *OLA1* may be highly related to cell proliferation and involved in tumor promoting and metastasis.

Subsequently, at the protein level, we established PPI networks of *OLA1*, which confirmed that *BRCA1*, *BRCA1*-associated RING domain protein 1 (*BARD1*) and *HSPA9* were closely correlated with *OLA1*. Breast and ovarian cancer risk may be increased by abnormal expression of *BRCA1* serving as a tumor suppressor gene. *BRCA1* forms a heterodimer with *BARD1* and functions in multiple cellular processes, including DNA repair and centrosome regulation. *OLA1* plays a significant part in the *BRCA1-BARD1*-mediated regulation of the centrosome. Studies showed that the loss of any of above three proteins caused centrosome amplification, which might contribute to chromosome instability and the promotion of cancer. Moreover, we found a link between *OLA1* and a number of well-known cancer-related pathway activities. The cell cycle pathways in *BRCA*, COAD, ESCA, KIRP, LUAD, LUSC, STAD, TGCT and THYM could be activated by increased *OLA1*. Further, we noted that *OLA1* expression had an impact on the activities of the RAS-Mitogen-Activated Protein Kinase (RASMAPK) pathway, DNA damage and apoptosis. The overall findings suggest that *OLA1* is

intimately engaged in the development of several tumors, indicating that *OLA1* may function as an oncogene in malignancies [66-73].

CONCLUSION

Our present study systematically analyzed the role of *OLA1* aberrant expression at different levels in pan-cancer, which was related to tumor promotion and patient prognosis. However, there are still some limitations in current study. Firstly, our pan-cancer study mainly based on the public databases and bioinformatics tools. The methods used to evaluate the data may potentially be inconsistent as a result of the data being in public databases from various sources, which could cause distinctions in the consequences. Secondly, there was no experimental support for our findings, which were primarily based on bioinformatics analyses. More biological experiments *in vitro* and *in vivo* are necessary to confirm the role of *OLA1* in malignancies.

In conclusion, our study first provides a comprehensive pan-cancer analysis of *OLA1*. We demonstrated that the aberrant expression of *OLA1* was correlated with patient outcomes, immune infiltrations, TMB, MSI, CNVs and DNA methylations in multiple cancer types. *OLA1* may therefore be a potential immunological and prognostic biomarker in pan-cancer.

REFERENCES

1. Sung H, Ferlay J, Siegel RL, Laversanne M, Soerjomataram I, Jemal A, et al. Global cancer statistics 2020: Global Cancer Observatory (GLOBOCAN) estimates of incidence and mortality worldwide for 36 cancers in 185 countries. CA Cancer J Clin. 2021;71(3):209-249.
2. Ribas A, Wolchok JD. Cancer immunotherapy using checkpoint blockade. Science. 2018;359(6382):1350-1355.
3. Gradia DF, Rau K, Umaki AC, de Souza FS, Probst CM, Correa A, et al. Characterization of a novel Obg-like ATPase (*OLA1*) in the protozoan Trypanosoma cruzi. Int J Parasitol. 2009;39(1):49-58.
4. Verstraeten N, Fauvart M, Versees W, Michiels J. The universally conserved prokaryotic GTPases. Microbiol Mol Biol Rev. 2011;75(3):507-542.
5. Koller-Eichhorn R, Marquardt T, Gail R, Wittinghofer A, Kostrewa D, Kutay U, et al. Human Obg-like ATPase (*OLA1*) defines an ATPase subfamily in the Obg family of GTP-binding proteins. J Biol Chem. 2007;282(27):19928-19937.
6. Matsuzawa A, Kanno SI, Nakayama M, Mochiduki H, Wei L, Shimaoka T, et al. The BReast CAncer gene 1 (*BRCA1*)/ *BRCA1* associated RING domain 1 (*BARD1*)-interacting protein Obg-like ATPase (*OLA1*) functions in centrosome regulation. Mol Cell. 2014;53(1):101-114.
7. Yoshino Y, Qi H, Fujita H, Shirota M, Abe S, Komiyama Y, et al. BReast CAncer gene 1 (*BRCA1*)-interacting protein Obg-like ATPase (*OLA1*) requires interaction with *BRCA1* associated RING domain 1 (*BARD1*) to regulate centrosome number. Mol Cancer Res. 2018;16(10):1499-14511.
8. Otsuka K, Yoshino Y, Qi H, Chiba N. The function of BReast CAncer gene 1(*BRCA1*) Associated RING Domain 1 (*BARD1*) in centrosome regulation in cooperation with *BRCA1*/ Obg-like ATPase (*OLA1*)/ Receptor for Activated C Kinase 1 (RACK1). Genes. 2020;11(8):842.
9. Sun H, Luo X, Montalbano J, Jin W, Shi J, Sheikh MS, et al. DOC45, a novel Deoxyribonucleic acid (DNA) damage-regulated nucleocytoplasmic Adenosine Triphosphate (ATPase) that is overexpressed in multiple human malignancies. Mol Cancer Res. 2010;8(1):57-66.
10. Liu J, Miao X, Xiao B, Huang J, Tao X, Zhang J, et al. Obg-like ATPase 1 enhances chemoresistance of breast cancer *via* activation of TGF-β/Smad axis cascades. Front Pharmacol. 2020;11:666.
11. Liu J, Yang Q, Xiao KC, Dobleman T, Hu S, Xiao GG. Obg-like ATPase 1 inhibited oral carcinoma cell metastasis through TGFβ/SMAD2 axis *in vitro*. BMC Mol Cell Biol. 2020;21:1-1.
12. Bai L, Yu Z, Zhang J, Yuan S, Liao C, Jeyabal PV, et al. Obg-like ATPase (*OLA1*) contributes to epithelial-mesenchymal transition in lung cancer by modulating the GSK3β/snail/E-cadherin signaling. Oncotarget. 2016;7(9):10402.
13. Dong Y, Yin A, Xu C, Jiang H, Wang Q, Wu W, et al. Obg-like ATPase (*OLA1*) is a potential prognostic molecular biomarker for endometrial cancer and promotes tumor progression. Oncol Lett. 2021;22(2):1-3.
14. Tomczak K, Czerwinska P, Wiznerowicz M. Review The Cancer Genome Atlas (TCGA): An immeasurable source of knowledge. Contemp Oncol (Pozn). 2015;2015(1):68-77.
15. Tang Z, Li C, Kang B, Gao G, Li C, Zhang Z. GEPIA: A web server for cancer and normal gene expression profiling and interactive analyses. Nucleic Acids Res. 2017;45(1):98-102.
16. Wang Q, Armenia J, Zhang C, Penson AV, Reznik E, Zhang L, et al. Unifying cancer and normal Ribonucleic Acid (RNA) sequencing data from different sources. Sci Data. 2018;5(1):1-8.
17. Asplund A, Edqvist PH, Schwenk JM, Ponten F. Antibodies for profiling the human proteome-The Human Protein Atlas (HPA) as a resource for cancer research. Proteomics. 2012;12(13):2067-2077.
18. Ru B, Wong CN, Tong Y, Zhong JY, Zhong SS, Wu WC, et al. Tumour Immune System Interaction Database (TISIDB): An integrated repository portal for tumor-immune system interactions. Bioinformatics. 2019;35(20):4200-4202.
19. Liu J, Lichtenberg T, Hoadley KA, Poisson LM, Lazar AJ, Cherniack AD, et al. An integrated The Cancer Genome Atlas (TCGA) pan-cancer clinical data resource to drive high-quality survival outcome analytics. Cell. 2018;173(2):400-416.
20. Liu CJ, Hu FF, Xia MX, Han L, Zhang Q, Guo AY. GSCALite: A web server for gene set cancer analysis. Bioinformatics. 2018;34(21):3771-3772.
21. Hanzelmann S, Castelo R, Guinney J. GSVA: Gene set variation analysis for microarray and RNA-seq data. BMC Bioinformatics. 2013;14:1-5.
22. Cerami E, Gao J, Dogrusoz U, Gross BE, Sumer SO, Aksoy BA, et al. The cBio cancer genomics portal: An open platform for exploring multidimensional cancer genomics data. Cancer Discov. 2012;2(5):401-404.
23. Bonneville R, Krook MA, Kautto EA, Miya J, Wing MR, Chen HZ, et al. Landscape of microsatellite instability across 39 cancer types. JCO Precis Oncol. 2017;1:1-5.
24. Schlattl A, Anders S, Waszak SM, Huber W, Korbel JO. Relating Copy Number Variation (CNV)s to transcriptome data at fine resolution: Assessment of the effect of variant size, type and overlap with functional regions. Genome Res. 2011;21(12):2004-2013.
25. Li B, Severson E, Pignon JC, Zhao H, Li T, Novak J, et al. Comprehensive analyses of tumor immunity: Implications for cancer immunotherapy. Genome Biol. 2016;17:1-6.
26. Li T, Fan J, Wang B, Traugh N, Chen Q, Liu JS, et al. Tumor Immune Estimation Resource (TIMER): A web server for comprehensive analysis of tumor-infiltrating immune cells. Cancer Research. 2017;77(21):108-110.
27. Miao YR, Zhang Q, Lei Q, Luo M, Xie GY, Wang H, et al. ImmuCellAI: A unique method for comprehensive T-cell subsets abundance prediction and its application in cancer immunotherapy. Adv Sci. 2020;7(7):1902880.
28. Siemers NO, Holloway JL, Chang H, Chasalow SD, Ross-MacDonald PB, Voliva CF, et al. Genome-wide association analysis identifies genetic correlates of immune infiltrates in solid tumors. PLoS One. 2017;12(7):e0179726.
29. Yoshihara K, Shahmoradgoli M, Martínez E, Vegesna R, Kim H, Torres-Garcia W, et al. Inferring tumour purity and stromal and immune cell

admixture from expression data. Nat Commun. 2013;4(1):2612.

30. Thorsson V, Gibbs DL, Brown SD, Wolf D, Bortone DS, Yang TH, et al. The immune landscape of cancer. Immunity. 2018;48(4):812-830.
31. Zeng Z, Wong CJ, Yang L, Ouardaoui N, Li D, Zhang W, et al. Tumor Immune Syngeneic MOuse (TISMO): Syngeneic mouse tumor database to model tumor immunity and immunotherapy response. Nucleic Acids Res. 2022;50(D1):D1391-D1397.
32. Szklarczyk D, Gable AL, Nastou KC, Lyon D, Kirsch R, Pyysalo S, et al. The Search Tool for the Retrieval of Interacting Genes/Proteins (STRING) database in 2021: Customizable protein-protein networks and functional characterization of user-uploaded gene/measurement sets. Nucleic Acids Res. 2021;49(D1):D605-D612.
33. Warde-Farley D, Donaldson SL, Comes O, Zuberi K, Badrawi R, Chao P, et al. The Gene Multitasker for Analysis of Networks and Interactions (GeneMANIA) prediction server: Biological network integration for gene prioritization and predicting gene function. Nucleic Acids Res. 2010;38(suppl-2):W214-W220.
34. Franz M, Rodriguez H, Lopes C, Zuberi K, Montojo J, Bader GD, et al. Gene Multitasker for Analysis of Networks and Interactions (GeneMANIA) update 2018. Nucleic Acids Res. 2018;46(W1):W60-W64.
35. Akbani R, Ng PK, Werner HM, Shahmoradgoli M, Zhang F, Ju Z, et al. A pan-cancer proteomic perspective on the cancer genome atlas. Nat Commun. 2014;5(1):3887.
36. Choucair K, Morand S, Stanbery L, Edelman G, Dworkin L, Nemunaitis J. Tumor Mutational Burden (TMB): A promising immune-response biomarker and potential spearhead in advancing targeted therapy trials. Cancer Gene Ther. 2020;27(12):841-853.
37. van Velzen MJ, Derks S, van Grieken NC, Mohammad NH, van Laarhoven HW. Microsatellite Instability (MSI) as a predictive factor for treatment outcome of gastroesophageal adenocarcinoma. Cancer Treat Rev. 2020;86:102024.
38. Leipe DD, Wolf YI, Koonin EV, Aravind L. Classification and evolution of P-loop GTPases and related ATPases. J Mol Biol. 2002;317(1):41-72.
39. Huang S, Zhang C, Sun C, Hou Y, Zhang Y, Tam NL, et al. Obg-like ATPase 1 (*OLA1*) overexpression predicts poor prognosis and promotes tumor progression by regulating P21/CDK2 in hepatocellular carcinoma. Aging. 2020;12(3):3025.
40. Liu Y, Kong XX, He JJ, Xu YB, Zhang JK, Zou LY, et al. Obg-like ATPase (*OLA1*) promotes colorectal cancer tumorigenesis by activation of HIF1α/CA9 axis. BMC Cancer. 2022;22(1):424.
41. Zhivotovsky B, Kroemer G. Apoptosis and genomic instability. Nat Rev Mol Cell Biol. 2004;5(9):752-762.
42. Nakamura Y. Deoxyribonucleic acid (DNA) variations in human and medical genetics: 25 years of my experience. J Hum Genet. 2009;54(1):1-8.
43. Liang L, Fang JY, Xu J. Gastric cancer and gene copy number variation: Emerging cancer drivers for targeted therapy. Oncogene. 2016;35(12):1475-1482.
44. Mace A, Kutalik Z, Valsesia A. Copy number variation. Methods Mol Biol. 2018:231-258.
45. Graf RP, Eskander R, Brueggeman L, Stupack DG. Association of copy number variation signature and survival in patients with serous ovarian cancer. JAMA Network Open. 2021;4(6):e2114162.
46. Kulis M, Esteller M. Deoxyribonucleic acid (DNA) methylation and cancer. Adv Genet. 2010;70:27-56.
47. Klutstein M, Nejman D, Greenfield R, Cedar H. Deoxyribonucleic acid (DNA) methylation in cancer and aging. Cancer Res. 2016;76(12):3446-3450.
48. Fumet JD, Truntzer C, Yarchoan M, Ghiringhelli F. Tumour mutational burden as a biomarker for immunotherapy: Current data and emerging concepts. Eur J Cancer. 2020;131:40-50.
49. Jardim DL, Goodman A, de Melo Gagliato D, Kurzrock R. The challenges of tumor mutational burden as an immunotherapy biomarker. Cancer Cell. 2021;39(2):154-173.
50. Luchini C, Bibeau F, Ligtenberg MJ, Singh N, Nottegar A, Bosse T, et al. European Society for Medical Oncology (ESMO) recommendations on microsatellite instability testing for immunotherapy in cancer and its relationship with Programmed cell Death Protein 1 (PD-1)/ Programmed Death Ligand 1 (PD-L1) expression and tumour mutational burden: A systematic review-based approach. Ann Oncol. 2019;30(8):1232-1243.
51. Chalmers ZR, Connelly CF, Fabrizio D, Gay L, Ali SM, Ennis R, et al. Analysis of 100,000 human cancer genomes reveals the landscape of tumor mutational burden. Genome Med. 2017;9:1-4.
52. Goodman AM, Sokol ES, Frampton GM, Lippman SM, Kurzrock R. Microsatellite-stable tumors with high mutational burden benefit from immunotherapy. Cancer Immunol Res. 2019;7(10):1570-1573.
53. Wu T, Dai Y. Tumor microenvironment and therapeutic response. Cancer Lett. 2017;387:61-68.
54. Lei X, Lei Y, Li JK, Du WX, Li RG, Yang J, et al. Immune cells within the tumor microenvironment: Biological functions and roles in cancer immunotherapy. Cancer Lett. 2020;470:126-133.
55. Sahai E, Astsaturov I, Cukierman E, DeNardo DG, Egeblad M, Evans RM, et al. A framework for advancing our understanding of cancer-associated fibroblasts. Nat Rev Cancer. 2020;20(3):174-186.
56. Biffi G, Tuveson DA. Diversity and biology of cancer-associated fibroblasts. Physiol Rev. 2020;101(1):147-176.
57. Zeltz C, Primac I, Erusappan P, Alam J, Noel A, Gullberg D. Cancer-associated fibroblasts in desmoplastic tumors: Emerging role of integrins. Semin Cancer Biol. 2020;62:166-181.
58. Kobayashi H, Gieniec KA, Lannagan TR, Wang T, Asai N, Mizutani Y, et al. The origin and contribution of cancer-associated fibroblasts in colorectal carcinogenesis. Gastroenterology. 2022;162(3):890-906.
59. Musa M, Ali A. Cancer-associated fibroblasts of colorectal cancer and their markers: Updates, challenges and translational outlook. Future Oncol. 2020;16(29):2329-2344.
60. Rhim AD, Oberstein PE, Thomas DH, Mirek ET, Palermo CF, Sastra SA, et al. Stromal elements act to restrain, rather than support, pancreatic ductal adenocarcinoma. Cancer Cell. 2014;25(6):735-747.
61. Ozdemir BC, Pentcheva-Hoang T, Carstens JL, Zheng X, Wu CC, Simpson TR, et al. Depletion of carcinoma-associated fibroblasts and fibrosis induces immunosuppression and accelerates pancreas cancer with reduced survival. Cancer Cell. 2014;25(6):719-734.
62. Huang H, Wang Z, Zhang Y, Pradhan RN, Ganguly D, Chandra R, et al. Mesothelial cell-derived antigen-presenting cancer-associated fibroblasts induce expansion of regulatory T cells in pancreatic cancer. Cancer Cell. 2022;40(6):656-763.
63. Ohlund D, Handly-Santana A, Biffi G, Elyada E, Almeida AS, Ponz-Sarvise M, et al. Distinct populations of inflammatory fibroblasts and myofibroblasts in pancreatic cancer. J Exp Med. 2017;214(3):579-596.
64. Xiang X, Niu YR, Wang ZH, Ye LL, Peng WB, Zhou Q. Cancer-associated fibroblasts: Vital suppressors of the immune response in the tumor microenvironment. Cytokine Growth Factor Rev. 2022;67:35-48.
65. Lu S, Han L, Hu X, Sun T, Xu D, Li Y, et al. N6-methyladenosine reader IMP2 stabilizes the ZFAS1/ Obg-like ATPase (*OLA1*) axis and activates the Warburg effect: Implication in colorectal cancer. J Hematol Oncol. 2021;14:1-23.
66. Miki Y, Swensen J, Shattuck-Eidens D, Futreal PA, Harshman K, Tavtigian S, et al. A strong candidate for the breast and ovarian cancer susceptibility gene BReast CAncer gene 1 (*BRCA1*). Science. 1994;266(5182):66-71.
67. Chen S, Parmigiani G. Meta-analysis of BReast CAncer gene 1 (*BRCA1*) and BReast CAncer gene 2 (*BRCA2*) penetrance. J Clin Oncol.

2007;25(11):1329-1333.

68. Wu LC, Wang ZW, Tsan JT, Spillman MA, Phung A, Xu XL, et al. Identification of a Really Interesting New Gene (RING) protein that can interact *in vivo* with the BReast CAncer gene 1 (*BRCA1*) gene product. Nat Genet. 1996;14(4):430-440.

69. Tarsounas M, Sung P. The antitumorigenic roles of BReast CAncer gene 1 (*BRCA1*)-*BRCA1* associated RING domain 1 (*BARD1*) in Deoxyribonucleic Acid DNA repair and replication. Nat Rev Mol Cell Biol. 2020;21(5):284-299.

70. Zhao W, Wiese C, Kwon Y, Hromas R, Sung P. The BReast CAncer gene (*BRCA*) tumor suppressor network in chromosome damage repair by homologous recombination. Annu Rev Biochem. 2019;88(1):221-245.

71. Xu X, Weaver Z, Linke SP, Li C, Gotay J, Wang XW, et al. Centrosome amplification and a defective G2-M cell cycle checkpoint induce genetic instability in BReast CAncer gene 1 (*BRCA1*) exon 11 isoform-deficient cells. Mol Cell. 1999;3(3):389-395.

72. McCarthy EE, Celebi JT, Baer R, Ludwig T. Loss of BReast CAncer gene 1 (*BRCA1*) associated RING domain 1 (*BARD1*), the heterodimeric partner of the *BRCA1* tumor suppressor, results in early embryonic lethality and chromosomal instability. Mol Cell Biol. 2003;23(14):5056-5063.

73. Yoshino Y, Fang Z, Qi H, Kobayashi A, Chiba N. Dysregulation of the centrosome induced by BReast CAncer gene 1 (*BRCA1*) deficiency contributes to tissue-specific carcinogenesis. Cancer Sci. 2021;112(5):1679-1687.